Alex Woolfe

303604

The stratigraphy and metamorphic facies of the Kel Enguef metamorphic belt near Gorom Gorom, NE Burkina Faso.

Supervisor: Prof. Kim A.A Ncube-Hein

Abstract

The Kel Enguef metamorphic belt is host to metamorphosed clastic and chemical sedimentary rocks that are intruded by gabbro dykes and a diorite pluton. The metamorphosed clastic and sedimentary rocks were deposited in a deltaic setting into a shallow marine environment. The sequences comprise fine- to coarse-grained sedimentary rocks that exhibit an overall upward coarsening stratigraphy. The metamorphism and deformation of the sequences is interpreted to have occurred mainly as a result of burial. Both greenschist and amphibolite grade metamorphism have been recognised. Gradation between these two facies is not observed. An anomalous occurrence of localised migmatite, which has attained granulite facies, lies between the greenschist and amphibolite and adds complexity to the metamorphic belt. The tectonic history of the region leads to further complexity of the KEMB. Folding and tectonic uplift are linked to regional deformation and the emplacement of local plutons. Indications of mineralisation occur in the form of an iron stone, ferruginous quartzite and a quartz-tourmaline vein. These raise interest for further research into possible large deposits of such kinds.

Table of Contents

1. Introduction

1.1 Preamble

The Kel Enguef metamorphic belt (KEMB) is located in the low hills southeast of Gorom Gorom, in the northeast of Burkina Faso. It is named after the village of Kel Enguef which is situated in the east of the field area. During field reconnaissance in 2010, the KEMB was found by the Wits research team where it presented an anomaly on the regional topographical and geological maps. The KEMB has not been researched in detail, thus how it fits in with the surrounding area is unknown. The general region of the KEMB has been mapped by Castaing et al. (2003) and the area has been shown to comprise basalt, rhyolite and tuffaceous material with evidence of possible gold mineralisation. Apart from Castaing et al. (2003) nothing further has been described for the area indicating the importance of this study. Studies in the surrounding area of the Oudalan-Gorouol Greenstone Belt (just east of the KEMB) by Nikiema et al. (1993), Pons et al. (1995), Debat et al. (2003), Tshibubudze et al. (2009) and Tshibubudze and Hein (submitted) give an understanding of the stratigraphic sequences and metamorphism in the area. This has given some indication of what might be present in the Kel Enguef metamorphic belt.

The project has involved the geological mapping of the field area with follow up petrographic and mineralogical work to elucidate the stratigraphy and metamorphic facies of the KEMB. An attempt has been made to reconstruct the environment of deposition and the tectonic setting. The study will also investigate if there is any economic mineralization and if so what type. The Essakane gold mine and Tambão manganese deposit are situated approximately 20km ESE and 40km NNE of the field area, respectively, and similar styles of mineralisation may occur in the field area.

1.2 Location and physiography

The KEMB is located in the northeast of Burkina Faso, approximately 275km to the northeast of Ouagadougou and east of the town of Gorom Gorom (Fig. 1.1a & 1.1b).

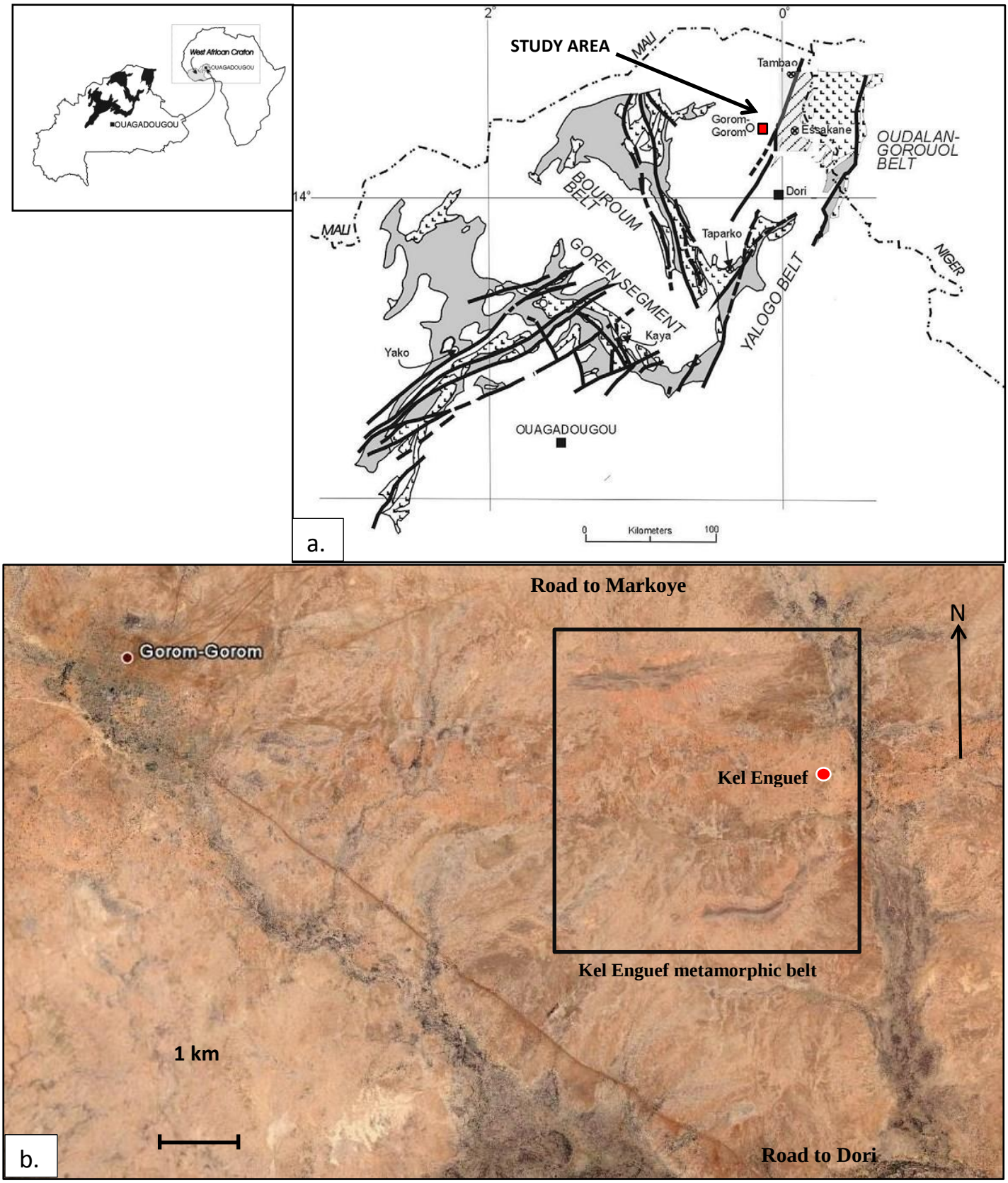

Figure 1.1: a) Location of field area within Burkina Faso with surrounding greenstone belts and major shears indicated (after Tshibubudze et al., 2009). b) Satellite image of the field area in relation to Gorom Gorom. Indicated on the image is the location of Kel Enguef and the main roads in the area. (Google Earth)

The field area, which is approximately 30km^2, hosts two east-west trending ridges that expose a portion of the KEMB (Fig. 1.1b). The UTM coordinates of the extent of the field area are: 30 P (Northern Hemisphere) 0805000 E, 1600000 N; 0805000 E, 1594000 N; 0810000 E, 1594000 N; 0810000 E, 1600000 N. This region of Burkina Faso is situated in the Sahel, just south of the Sahara Desert. Climatic conditions are arid, that is very hot and dry. Field work was carried out in January which is the coolest time of the year although daily temperatures exceeded 30 ^{0}C. Wind speeds are typically high which provided some relief from the heat. These winds, however, can cause a lot of dust to rise. At this time of the year, the dust forms what is called the pre-Harmattan.

The land between the ridges and on either side is relatively flat with river channels cutting into the land. The river channels are narrow and dissect the land surface to a metre depth making traveling by vehicle difficult. At this time of the year water is becoming increasingly scarce and all rivers in the region are now dry. River channels trend east towards a major river that is located on the eastern limits of the field area. The majority of the land between the ridges is covered by millet fields where the underlying rock is covered by a layer of sand. Huts are scatted across the farm land with the village of Kel Enguef situated to the east between the two ridges of the field area (Fig. 1.1b). Dirt roads are present connecting the village of Kel Enguef to the main road off to the west of the field area. Access into the field was either from this main road or from the north off a main road that connects Gorom Gorom to the village of Markoye (Fig. 1.1b).

1.3 Aims

The KEMB had not previously been mapped in detail and no previous research has been done on the area. This project attempted to gain a better understanding of the geology of the area with a focus on the stratigraphy and metamorphism. The environment of deposition of the rocks was determined. The pressure and temperature conditions were established to determine the metamorphic grade and the overall metamorphic history of the KEMB. An economic aspect in this project was to study mineralisation present in the KEMB if any.

1.4 Acronyms

KEMB- Kel Enguef metamorphic belt

UTM- Universal Transverse Mercator

TTG- Tonalite-trondjhemite-granodiorite

2. Geology setting

2.1 Regional geology and tectonics

The West African Craton is composed of Palaeoproterozoic rocks of the Birimian Supergroup (Feybesse et al., 2006; Hein, 2010) and Tarkwa Group (Davis et al., 1994) as well as calc-alkaline plutons which include tonalite-trondjhemite-granodiorite and diorite intrusions which intrude the Palaeoproterozoic stratigraphy (Pons et al., 1995; Naba et al., 2004 Hein, 2010). The Birimian Supergroup is dominated by metamorphosed sedimentary, volcano-sedimentary and volcanic sequences. The meta-volcanic sequences in the Goren greenstone belt and Boromo greenstone belt are at dated at 2238 ± 5 Ma and 2171 ± 7 Ma respectively (Castaing et al., 2003) based on Pb-Pb zircon dating from rhyolites within the belts. The metasedimentary rocks of the Birimian Supergroup comprise mainly metamorphosed volcaniclastics, greywacke, siltstone, shale, chemical sediments and chert. The younger Tarkwa Group, dated at 2194–2132 Ma from U-Pb detrital zircons (Davis et al., 1994), comprises clastic sedimentary rocks derived from erosion of the Birimian Supergroup of which it overlies unconformably (Hirdes et al., 1992 and Davis et al., 1994).

The craton has been subjected to several tectonic events corresponding to the deformation of Birimian Supergroup. This includes the SW directed shortening of the Tangaean Event (2170-2130 Ma), SE-NW shortening of the Eburnean Orogeny (2130-1980 Ma) and the young Wabo-Tampelse Event. The Tangaean Event and Eburnean Orogeny were associated with emplacement of TTG-suite plutons and dykes (Feybesse et al., 2006; Tshibubudze et al., 2009; Hein 2010). The tectonic events resulted in the formation of greenstone belts separated by the granitoids (Hirdes and Davis, 2002). The Eburnean Orogeny resulted in regional metamorphism of the Birimian Supergroup to greenschist facies and contact metamorphism from pluton emplacement to low - medium amphibolite facies (Pons et al., 1995; Debat et al., 2003).

2.2 Local geology

The Markoye Shear Zone lies to the east of the KEMB. The Oudalan-Gorouol Greenstone Belt is situated just east of the shear zone (Pons et al., 1995; Tshibubudze et al., 2009; Tshibubudze and Hein, submitted). This comprises metamorphosed and deformed

volcaniclastic, volcanics and sedimentary rocks. The sedimentary units are composed of metamorphosed conglomerate, quartzite, greywacke, siltstone, shale and chemical sedimentary rocks (Nikiéma, 1992; Pons et al., 1995; Tshibubudze et al., 2009; Tshibubudze and Hein, submitted). Volcaniclastic sequences comprise greywacke composed of medium-grained quarts and feldspar-rich sand. Intercalated with greywacke units are fuchsite layers, thin chert beds, shale, siltstone and rare pebble beds (Pons et al., 1995; Tshibubudze et al., 2009). A calk-alkaline series comprising ultramafics, gabbro, basalt, andesite and rhyolite associated with the volcaniclastic and sedimentary rocks are present (Pons et al., 1995)

Two phases of regional metamorphism are present in these rocks and characterised by two mineral assemblages (Pons et al., 1995). These are low-grade assemblages of prehinite, chlorite, actinolite and quartz as well as low-grade assemblages associated with regional schistosity. Specifically the Oudalan-Gorouol Greenstone Belt has undergone greenschist-facies metamorphism (Tshibubudze et al., 2009). Regional metamorphism to greenschist facies is associated to north-south crustal shortening during the Eburnean Orogeny (Vidal et al., 1996, Beziat et al., 2000, Hein et al., 2004 and Naba et al., 2004). Contact metamorphism of these rocks occurred due to the emplacement of granitoids which include granite-adamellite, granite and granodiorite compositions (Pons et al., 1995; Debat et al., 2003; Tshibubudze et al., 2009). Metamorphism of the surrounding units to the granitoids occurred to amphibolite-facies (Pons et al., 1995; Tshibubudze et al., 2009; Tshibubudze and Hein, submitted) and granulite facies (Tshibubudze and Hein, submitted).. Through hornblende barometric estimates, shallow crust (3-4 kbar) emplacement of plutons has been established (Pons et al., 1992).

Gold and manganese mineralisation as well as pegamatite veins are present in the Oudalan-Gorouol greenstone belt (Milési et al., 1992; Nikiéma, 1992; Beauvais et al., 2008 Tshibubudze, et al., 2009; Tshibubudze and Hein, submitted). Gold mineralisation, found at many locations, is hosted in shear zones as structural hosted lode-gold associated with NW-SE structures (Nikiéma, 1992; Tshibubudze et al., 2009; Tshibubudze and Hein, submitted). Manganese mineralisation is situated NE and SW of the KEMB at Tambão and Billiata (Tshibubudze and Hein, submitted) and pegamatite veins are situated NE at Tambão.

3. Methodology

In order to gain an understanding of the field area, a mosaic was constructed using Google Earth® images of the Kel Enguef metamorphic belt before entering the field. This was used to locate the field area with respect to the surrounding topography which included the location and orientation of rivers and ridges, as well as roads and villages. These were used for orientation in the field.

Reconnaissance of the terrain and geology was carried out in the field area before mapping commenced. This assisted in planning field mapping and the location of suitable drop-off and pick-up points and access within the field area. Mapping was carried out over a period of 13 field days during January 2011. Field mapping was undertaken by 3 relatively straight northwest-southeast traverses directly across the field area, one on either side of the field area and one through the middle (Fig. 3.1). Multiple short traverses were carried out across each ridge running perpendicular to strike. Furthermore, loosely defined traverses were carried out in the central region and south of the southern ridge to locate outcrop which was scarce. Data was recorded in field books and notes were supported by photographs of selected outcrops along traverse lines. The location, rock type, attitude, mineralogy, structural data and metamorphism were recorded. Rock samples were taken at particular station points during mapping. Logging and back up of all data was done after each day in the field.

The Google Earth mosaic was geo-referenced using MapInfo. Station points that were situated at positions easily identified on the image were used as reference points in the geo-referencing process. Once the image was referenced using five such points, the remaining station points were overlaid onto the image (Fig. 3.1). This created an image overlaid with station points corresponding to their actual position. By overlaying tracing paper onto the image, geographical and geological features were recorded to produce a geographical and surface cover map (Fig. 3.2) as well as a geological map (Fig. 3.3). These traces were then digitized using CorelDraw®.

Samples were strategically selected for thin sections and polished ore blocks. An initial 15 samples were submitted to the Wits Geosciences Laboratory to be processed (14 thin sections and 1 polished ore block) in early March 2011. A further 25 samples were submitted to SGS for thin sections and XRD (samples with economic interest). Another 3 samples were

submitted to Wits Geosciences Laboratory for ore blocks in June 2011. Thin sections petrography analysed for mineral assemblages, grain size and textural features. Minerals were identified using their optical properties with the assistance of mineral identification books and knowledgeable staff members. Associations between minerals were also a focus. The petrographic data combined with field data was used to determine protoliths and metamorphic facies. Ore blocks were analysed for minerals present with the help of XRD data. Mineral associations were a focus in determining petrogenesis. Pictures were taken of the thin sections and ore blocks to indicate mineral assemblages and textural features present in the samples.

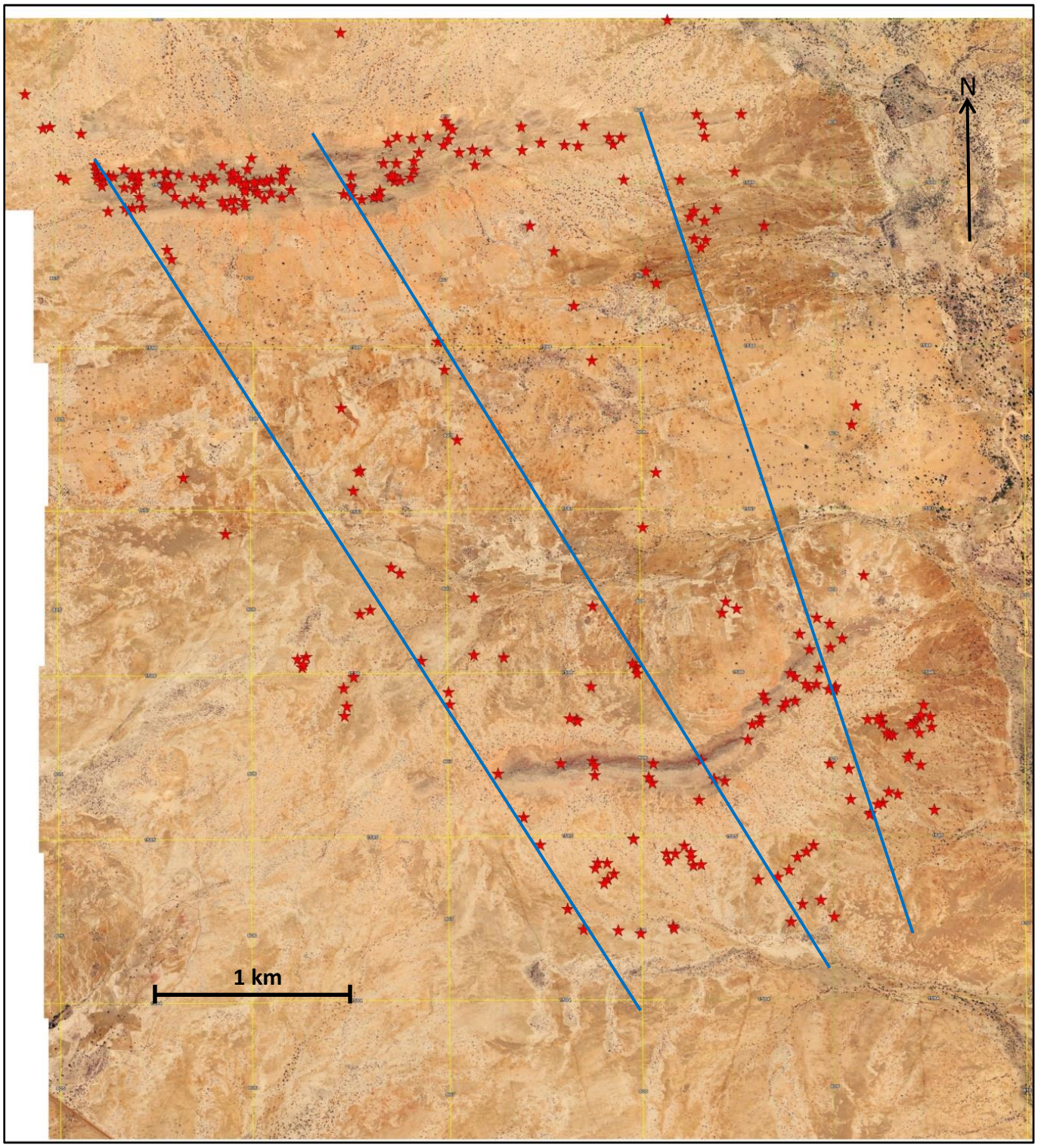

Figure 3.1: Google Earth mosaic of the KEMB with station point distribution and NW-SE traverses (blue lines) indicated over the field area. The ridges, central and southern region were mapped by loosely defined traverses.

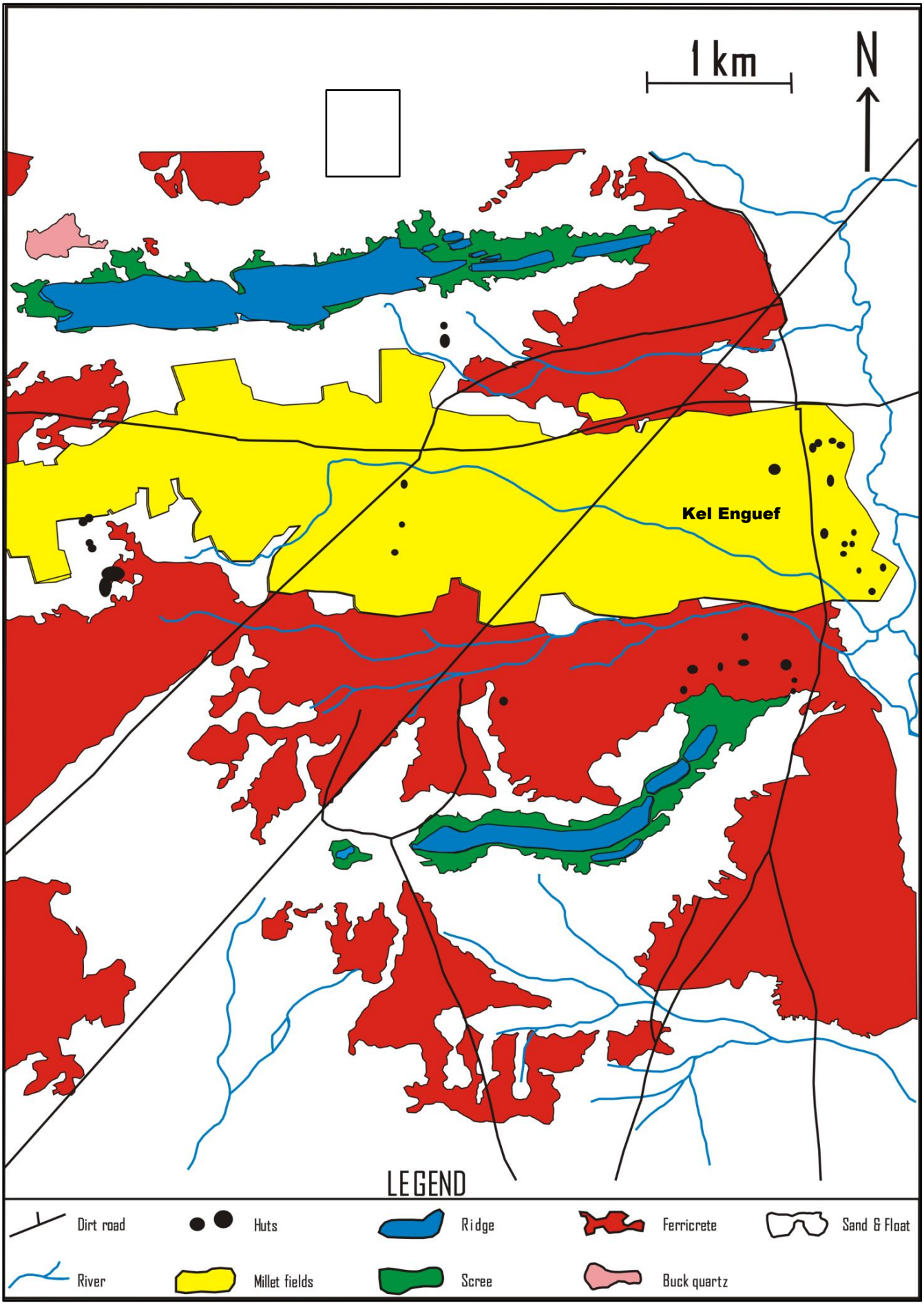

Figure 2.2: Geography and surface cover map of the KEMB.

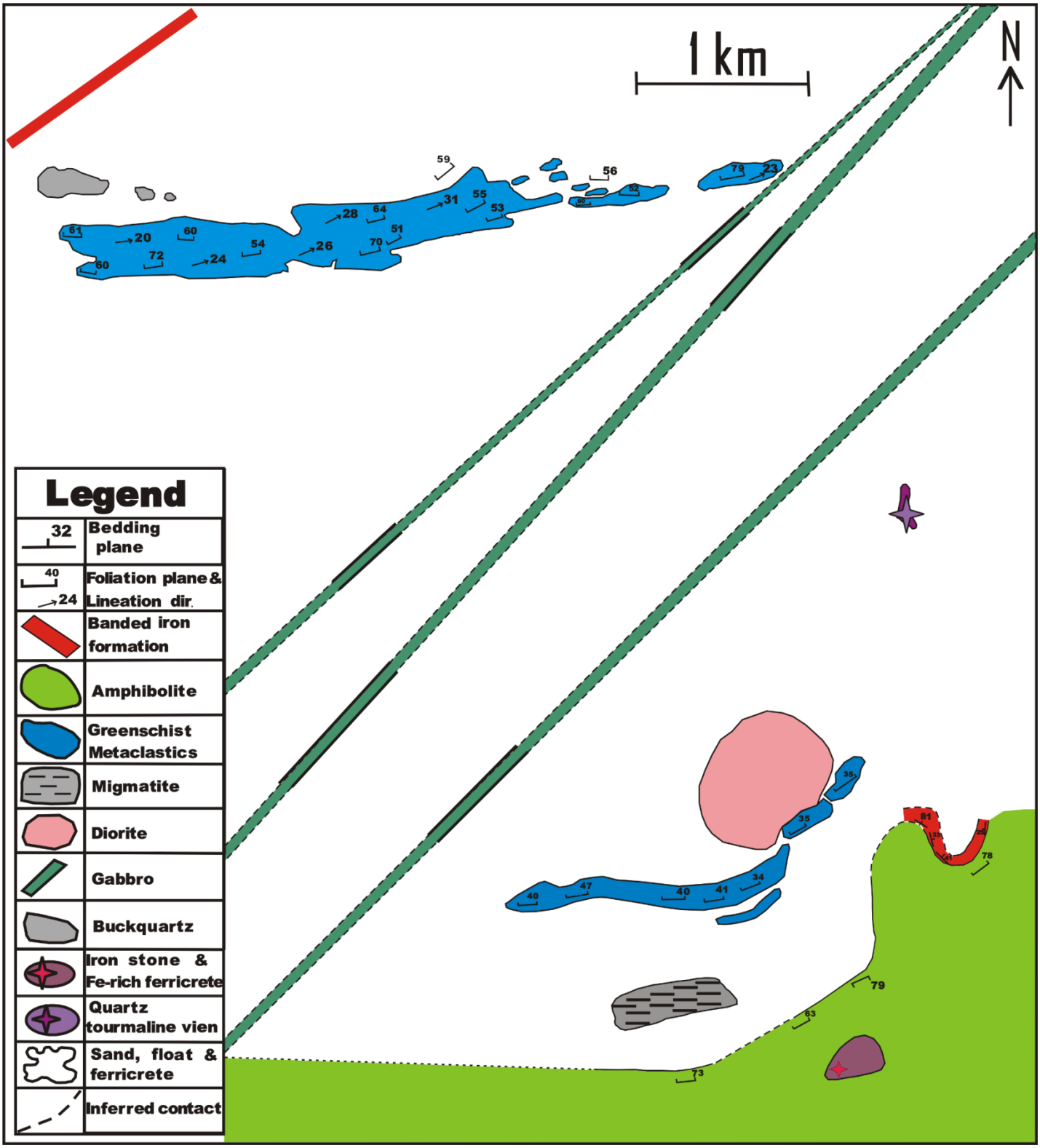

Figure 3.3: Geological interpretation map of the KEMB

4. Field description

The field area is a metamorphic terrane that ranges from greenschist facies to amphibolite facies, with metamorphic grade increasing from the north to the south. The two east-west trending ridges are host to greenschist facies rocks which are separated by relatively flat open millet fields with limited outcrop. The outcrop in this region indicates the presence of cross-cutting gabbro dykes, a dioritic pluton and possibly underlying greenschist facies, metamorphosed sedimentary rocks. Rocks of amphibolite facies are situated along the southern margin of the field area where the outcrop trends east west. Between the amphibolite zone and the southern ridge, outcrop is scarce however a localised pod of migmatite-gneiss occurs herein.

Mapping in the central and southern region was limited by the lack of outcrop. The region between the two ridges is approximately 3 km wide and comprises sandy farming land in the centre, as well as river beds which drain towards the east. Rock is present as sparse float. The regions between the farm land and ridges are covered by loose sand and float. Float is derived from the ridges. Buck quartz veins crop out near the margin of the two ridges; the veins are dark grey in colour. They have a lateral extent in an east-west direction. A characteristic of the veins is a dense network of fractures marked by black glass.

The northern part of the field area is host to an extensive fluvial system which was dry at the time of field work. The associated alluvial sediment covers the underlying rock apart from the western edge of the field area where small, low lying outcrops are visible. A large buck quartz vein is located 100 m north of the northern ridge.

4.1 Metamorphic stratigraphy

The southernmost region of the field area comprises amphibolite which crops out poorly. The amphibolite is dark green in colour and hosts a strong fabric that is pervasive. The sequence is medium- to fine-grained and dominated by hornblende and quartz. Course-grained hornblende-bearing quartzite occurs within the amphibolite (Fig. 4.1d), especially to the east of the sequence. The fabric is derived from compositional layering (Fig. 4.1a). Quartz layers are dominated by quartz with small amounts of hornblende, and plagioclase is absent. These layers are generally thinner than the hornblende layers. Hornblende layers are dominated by fine-grained hornblende and quartz with minor plagioclase. Fine compositional layering is found in the east where the unit is folded and contains small-scale shears (Fig. 4.1b & 4.1c).

Coarse-grained quartz-plagioclase veins cut the amphibolite and are also present along some shear zones. These veins are only seen in this part of the unit and are a few millimetres in width. Deformation is variable throughout the unit. Isoclinal folding (Fig. 4.1e), shearing and augen gneiss is common in the eastern part of the unit. Small scale isoclinal folds are present where limbs of the folds are close and within a fold width of 10 to 20 cm. Some isoclinal folds are truncated by small-scale planar shears. Slip was determined to be sinistral reverse. Augen gneiss are present with augen tails extend many centimetres away from each augen parallel to compositional banding (Fig. 4.1d). The augen are up to 2 cm thick and 5 cm long. Some augen exhibit a weak anticlockwise rotation.

These deformation features are confined to the east of the sequence where a large scale fold is located. Although the sequence cannot we traced continuously, the variable strike would suggest a large fold. Tracing the amphibolite outcrop from east to west, the fabric orientation is as follows: $019^0/70^0$W, $052^0/64^0$E, $051^0/78^0$W, $178^0/63^0$E, $008^0/75^0$E which sharply changes to $066^0/79^0$S.

To the west, the amphibolite has a relatively constant trend of about 075^0 dipping to the north at approximately 72^0. Deformation of the unit is less evident in the west. Here spotted amphibolite is present (Fig. 4.1f). Coarse-grained plagioclase crystals form positive weathering features that stand proud of the rock. The plagioclase crystals are about 4 mm in diameter and stand out approximately 2 mm from the surface. These give the spotted amphibolite its appearance.

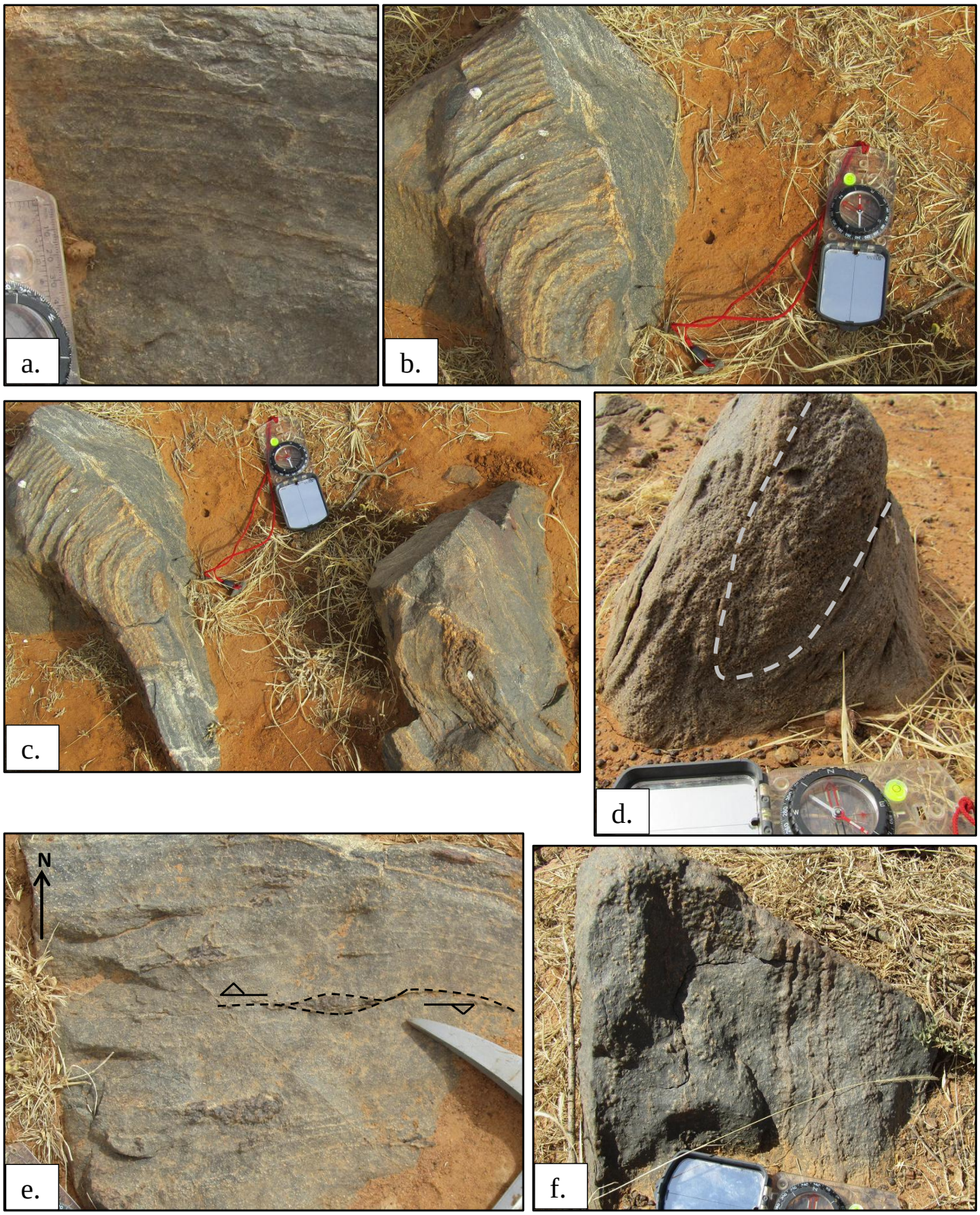

Figure 4.1: Amphibolite outcrop. a) fine composition-banding located in the eastern part of the units. b & c) small scale shear truncating isoclinal fold. d) small scale isoclinal fold in hornblende-baring quartzite. e) quartz augen with sinistral rotation. f) spotted amphibolite with compositional-banding.

Two layers of metamorphosed banded iron formation crop out on the eastern side of the field area just north of the amphibolite. The contact between the two units is not visible. Outcrop to subcrop can be traced for approximately 300 m. The banded iron formation comprises fine laminations (not more than 1 cm thick) of light grey chert and dark brown, fine-grained, ironstone (Fig. 4.2a). An irregular surface exists between the chert and iron-rich layers. Soft-sediment deformation features are evident by the presence of isoclinal slump folds (Fig. 4.2a). A common feature of the banded ironstone is cross-cutting thin, siliceous veins. The combination of the siliceous layers and veins create a cross-hatched pattern on weathering surfaces especially where veins are concentrated (Fig. 4.2b). The banded ironstone formation is folded. It changes in strike from 066^0 to 137^0 and 168^0 before abruptly turning to 069^0 (Fig. 3.3). The banded ironstone formation dips towards the north between 30 and 45^0. In the west of the region, banded ironstone float was observed over a distance of about 100 m. The float is scattered with no in-situ outcrop visible thus questioning whether the formation is present here.

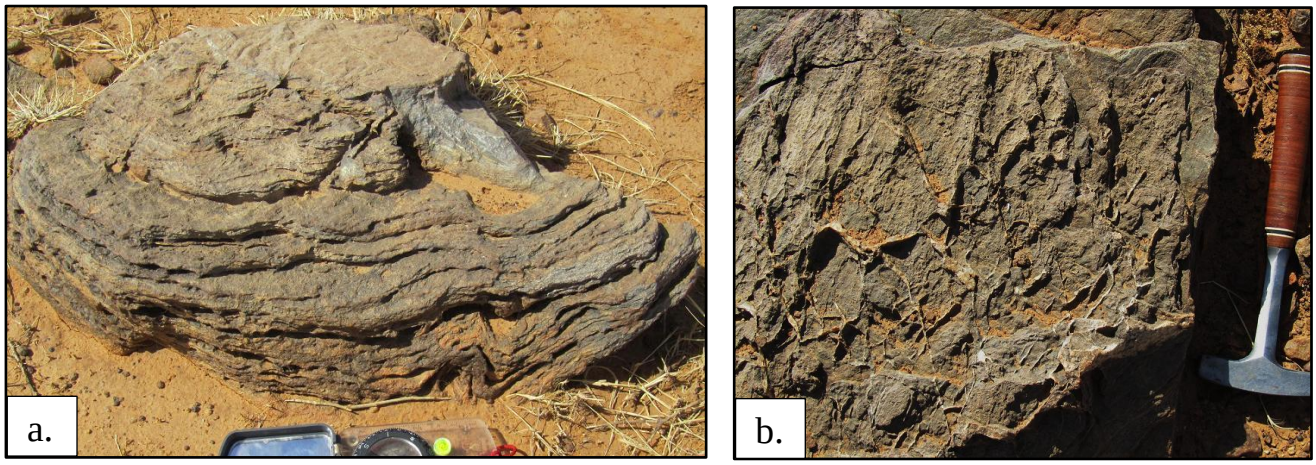

Figure 4.2: Banded ironstone. a) fine laminated banding with soft sediment slump folding. b) dense quartz veins exhibiting a cross-hatch weathering pattern.

The southern ridge is approximately 2.5 km in length trending east-west (in the west) and northeast-southwest (in the east). The eastern limb of the ridge has a mean calculated strike and dip of 066°/37°N (Fig. 4.3a). The western limb has mean calculated strike and dip of 270°/42°N (Fig. 4.3b) with orientation data fitting tightly together. The southern ridge comprises four quartz-rich units (Units A – D) of similar mineralogy that can be distinguished by varying grain size (and slight compositional variation). The southern units comprise isoclinal folds with hinges parallel to the bedding plane.

Unit A is a medium-grained quartzite that hosts fine-grained muscovite and iron oxides. Iron rich zones are not constrained to single beds. Hornblende occurs in lesser amounts in this unit and is seen as black specks in the rock. Unit A is discontinuous along the southern margin of the southern ridge. A small ridge that is located just south of the main ridge exposes the best outcrop of this unit. The unit is absent to the west of this ridge whereas to the east it is discontinuous. The quartzite strikes approximately 080^0 and dip towards the north at about 45^0. The grain size decreases northward towards Unit B.

Unit B consists of interbedded fine- and medium- grained, iron-rich quartzite that is dark red-brown in colour. The unit is approximately 10 m thick. Bedding features are not visible within the unit and compositional layering is not well presented.

Unit C is situated along the southern slope of the southern ridge and comprises a medium- to coarse-grained quartzite with muscovite, iron oxides and epidote. Unit C is gradational with Unit B and D. Within Unit C, there are zones with varying iron content. Compositional layering is prominent in this unit. Quartz grains are strained and elongated parallel to the direction of compositional layers. A fabric, parallel to compositional layers is pervasive throughout the unit (Fig. 4.5a & 4.5b). This unit it continuous along the southern slope of the ridge and coarsens towards the top of the ridge and Unit D.

The top of the ridge and the northern slope consist of coarse-grained quartzite with medium- to fine-grained muscovite, epidote, quartz and interstitial iron oxide (Unit D). Quartz grains are angular and elongated parallel to strike of compositional layers which are well defined in Unit D. Layers range from a few centimetres up to tens of centimetres. Quartz grains are course from 5 to 10 mm. Iron content varies throughout the unit. Some layers exhibit tight folds and undulations. This unit strikes approximately 090^0 and dips at 40^0 northward on the

western limb of the ridge. On the eastern limb of the ridge, the unit strikes at approximately 065^0 and dips 35^0 northward. The eastern limb is disjointed

A fine-grained, ferruginous-quartzite is located approximately 100 m away from the eastern end of the southern ridge. Outcrop is confined to a 20 m stretch with a width of 3 m. The unit is highly magnetic, massive and coarse-grained with dark red quartz veins crosscut the unit.

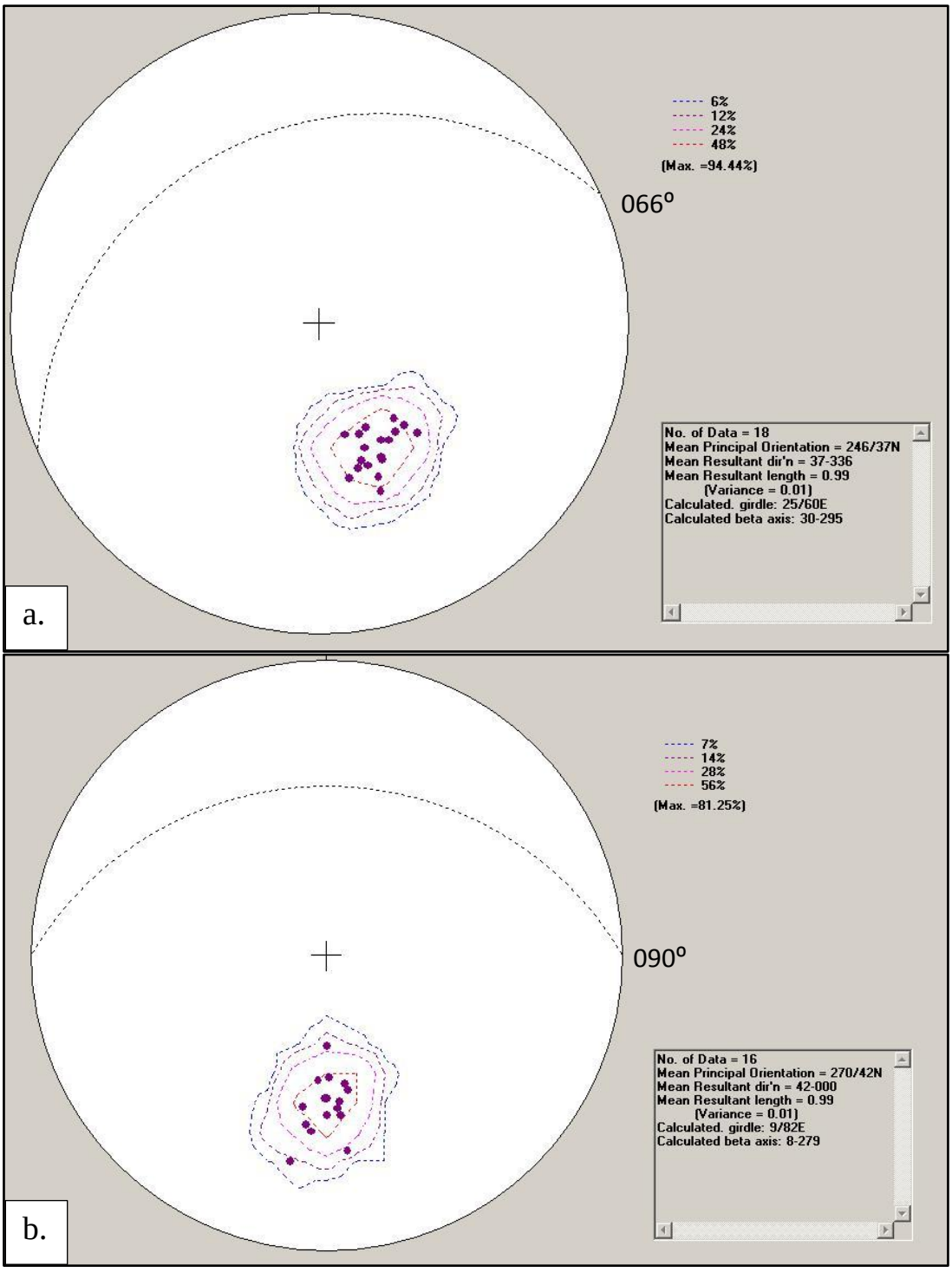

Figure 4.3: Equal area stereographic projection of poles to (a) the eastern limb of the southern ridge with a mean calculated strike and dip of 066°/37°N and (b) the western limb of the southern ridge with a mean calculated strike and dip of 090°/42°N.

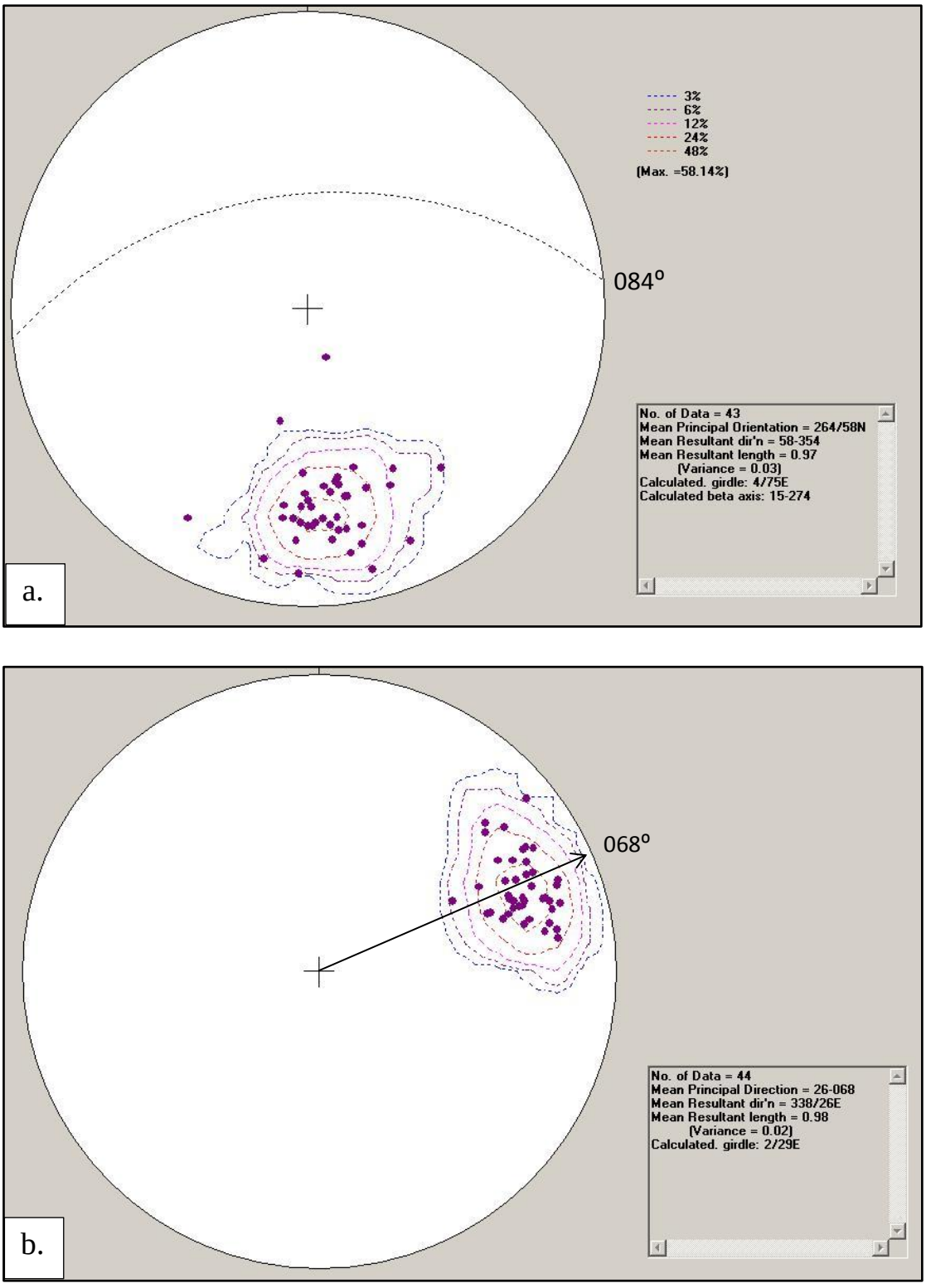

Figure 4.4: Equal area stereographic projection of (a) poles to the northern ridge with a mean calculated strike and dip of 084°/58°N and (b) the orientations of dominant lineations in the northern ridge with a mean calculated principle direction of 068°/26°.

The northern ridge consists of three meta-sedimentary units that are metamorphosed to greenschist facies. As with the southern ridge, the rocks here are dominated by quartz with muscovite, epidote and iron oxides. The central and western region of the northern ridge host three well defined units which form ridges separated by valleys. Here the units trends approximately east-west and dip at 58^0N (Fig. 4.4a; 4.5f & 4.5g). In the eastern region, the units are poorly defined and the ridges are broken up to form low hillocks where the units trend 085^0 and dip 60^0 N. A dominant lineation is common in the outcrop with a dip and dip direction of 26^0 towards 068^0 (Fig. 4.4b).

Unit X (southern side of the northern ridge), comprises a medium- to coarse-grained quartzite. Unit X is approximately 50 to 100 m thick. Compositional variations are evident throughout. It is common to have iron rich horizons, which are a dark red brown in colour and vary in thickness from 10 to 20 cm up to a few metres. Compositional layering is typically planar to undulate with a pervasive fabric parallel to layering (Fig. 4.5e). This unit is continuous in the central and western regions of the main ridge, but is crosscut by a series of north-westerly trending faults. Towards the eastern end of the ridge the faults off-set Unit W up to 40 m.

Unit Y (centre of the northern ridge) is dominated by course-grained quartzite with rare muscovite and iron oxides. Quartz pebbles range up to a few centimetres in size. The quartz grains are elongated and form a strong fabric in the unit. Quartz veins are present which are parallel to the fabric. These can range in size from a few centimetres in width and length up to several metres, showing little to no foliation through them.

Unit Z, located on the northern side of the northern ridge, comprised interbedded fine- to coarse-grained metapelite to quartzite. Where grain size is coarse, compositional layering is thick (up to 40 cm) with quartz pebbles up to 2 cm in size with varying amounts of muscovite and epidote. The iron content varies throughout the unit (Fig. 4.5c). Metaclastics exhibit thin bedding (on a centimetre scale) with quartz grains up to 2 mm in size and accessory muscovite and epidote. A high concentration of iron oxide is present in layers. Quartzite beds are typically thicker with pebbles up to 10 mm in size. Muscovite is more abundant in these beds. The unit exhibits strained grains that are elongated parallel to bedding and gives rise to grain lineation. Quartz veins are a common feature and are occur parallel to bedding with crystal growth perpendicular to bedding.

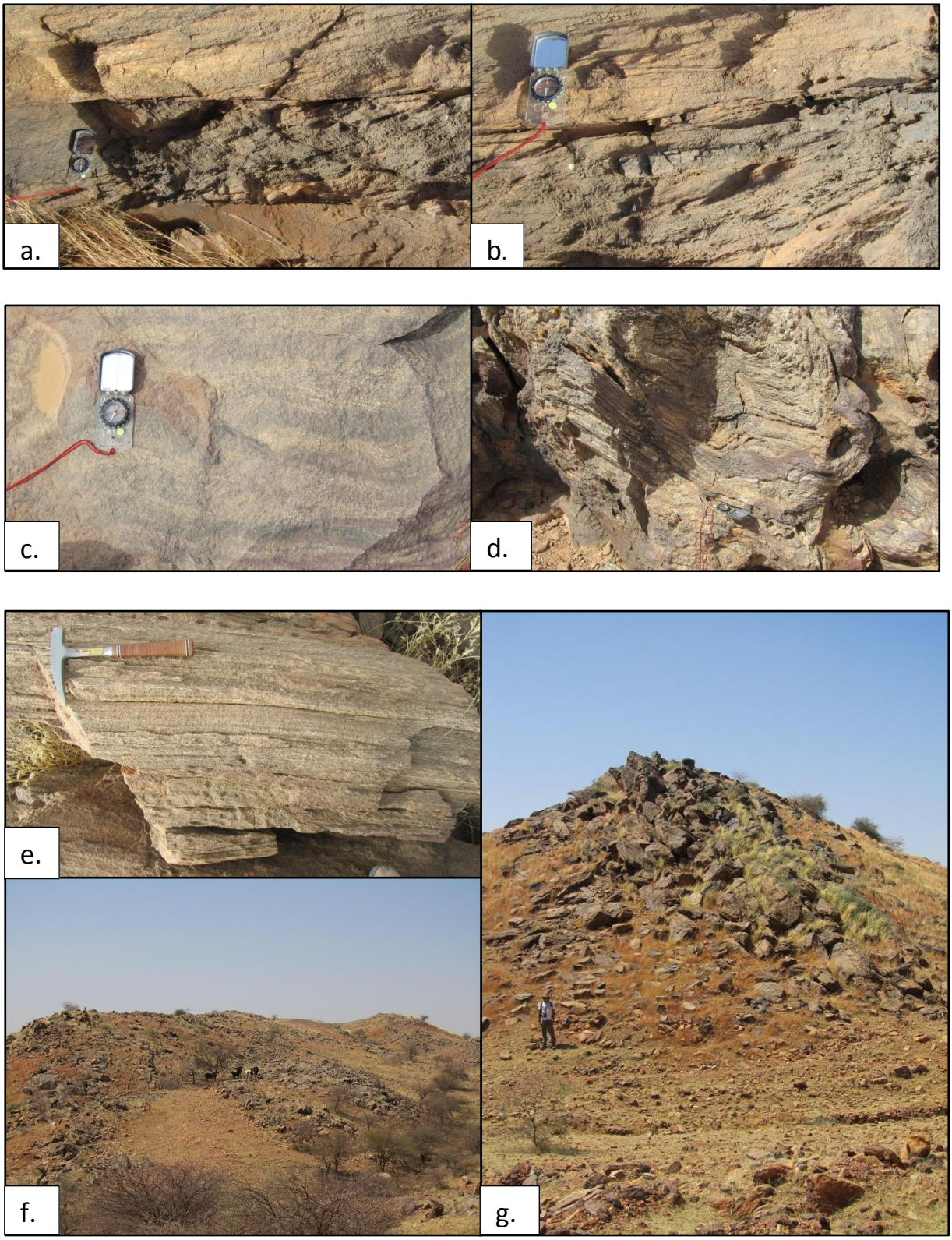

Figure 4.5: Greenschist facies rocks. a & b) bedding with subparallel to parallel foliation. c) iron-rich (dark) and iron-poor (light) layering in fine-grained metaclastic. d) highly foliated and deformed beds of the southern ridge. e) strong foliation in medium-grained beds. f & g)moderately northerly dipping beds of the northern ridge.

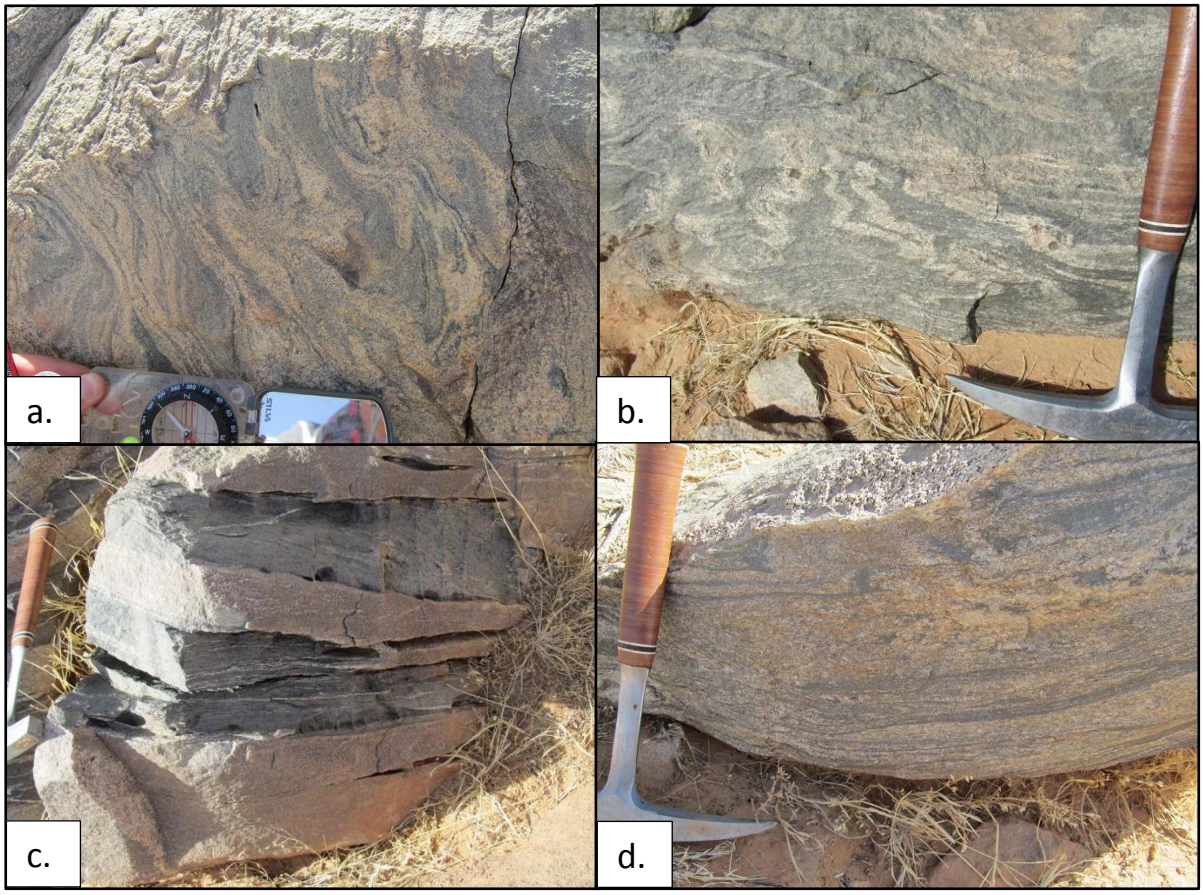

Figure 4.6: Migmatite-gneiss outcrop exhibiting (a & b) fine compositional bands with flow textures, (c) thick compositional bands of leucosomes and melanosomes and (d) regions of gneissic textures.

A zone of migmatite-gneiss crops out in the south of the field area between amphibolite and greenschist facies rocks. Outcrop occurs as large boulders and in-situ blocks which are scattered over an area covering about 600 by 200 m (Fig. 3.3). Over the full extent of the outcrop there is large variation between zones of migmatite and gneiss. The migmatite contains compositional bands of dark and light grey minerals that characterise partial melt with flow texture. The compositional bands vary from a few millimetres in thickness to many centimetres (Fig. 4.6a & 4.6b) and less commonly up to approximately 20 cm thick (Fig. 4.6c). The light coloured bands consist of medium- to fine-grained quartz, plagioclase, alkali feldspar and accessory muscovite and biotite. Dark grey bands are fine-grained and consist of biotite and quartz with accessory plagioclase. The gneissic zones exhibit partial zoning of light and dark minerals (Fig. 4.6d). The gneiss consists of medium- to course-grained quartz, plagioclase, alkali feldspar and mica. Within in the gneiss there are potassium rich zones which are observed where the outcrop has a grey-pink appearance. Veins of coarse-grained quartz and plagioclase cross cut the migmatite and gneiss with some exhibiting off set. The veins are orientated north-south.

4.2 Ferricrete

The flat lying area is covered by ferricrete which is made up of two horizons (Fig. 4.7). The most prominent outcrops occur around the southern ridge and in the north east of the field area. The best exposure occurs where rivers have cut into these outcrops. The upper horizon is approximately 1 m thick and the lower is about 20 cm thick. The dark red ferricrete horizons consist of quartz-iron pisoliths in an iron-cement comprising haematite and goethite.

Figure 4.7: Ferricrete horizons in river cutting

4.3 Tertiary sands

These lie above the ferricrete horizons and sometimes as perched ridges on the sides of the main ridges. The sands are currently eroding.

4.4 Intrusions

A diorite pluton crops out poorly on the northern side of the southern ridge in contact with greenschist facies meta-sedimentary rocks. The diorite is light grey in colour and consists of, quartz, plagioclase and muscovite. The pluton is roughly oval in shape.

Gabbro dykes are interpreted to crosscut the central region between the northern and southern ridges. This is based on a linear array of gabbro in subcrop across the region and coincident linear magmatic highs in geophysical maps of the region. Boulders of gabbro are commonly located several metres to hundred metres apart from one another, but a 6 m wide northeast trending outcrop of gabbro is situated on the north-western side of the southern ridge. Outcrops of gabbro were observed near houses and on tracks. The outcrop consisted of medium-grained crystals of plagioclase and pyroxene. Distribution of minerals is homogeneous. Quartz veins crosscut the gabbro. Where the quartz veins are thin (between 5 and 10 mm) the quartz is isotropic and where the veins are thicker (up to 50 mm) large quartz crystals are present. The width and lateral extent of the dykes is not well defined due to the lack of outcrop. It is determined that at least three dykes cross-cut the central region.

4.4 Mineralisation indicators

Iron occurrence

A fine-grained, ferruginous-quartzite (Fig. 4.8) is located approximately 100 m away from the eastern end of the southern ridge. Outcrop is confined to a 20 m stretch with a width of 3 m. The unit is highly magnetic, massive and coarse-grained with dark red quartz veins crosscut the unit.

An iron stone is hosted in the amphibolite, situated in the southern most region of the field area. It is black in colour, extremely hard and strongly magnetic. It is fine-grained and crosscut by 10 cm thick quartz veins (Fig. 4.9b & 4.9c). The outcrop is 3 m in size (Fig. 4.9a). Iron-rich ferricrete surrounds the outcrop.

Quartz-tourmaline vein

A massive quartz tourmaline vein is situated approximately a kilometre northeast of the diorite. This vein is 30 m long and sigmoidal in form. Therein hosts an abundance of tourmaline crystals that are randomly orientated (Fig. 4.10a). The crystals are up to 3 cm in length and 3 mm in width. Tourmaline veins (approximately 20 cm) crosscut the quartz vein with tourmaline crystals extending out from veins (Fig. 4.10b). The tourmaline veins strike 170^0 and dip 20^0 E.

Figure 4.8: Fine-grained, ferruginous-quartzite cut by quartz vein (left)

Figure 4.9: (a) Localised iron stone outcrop which (b) comprises dark-red, fine-grained iron-rich minerals (c) cross-cut but quartz veins and cataclastic quartz.

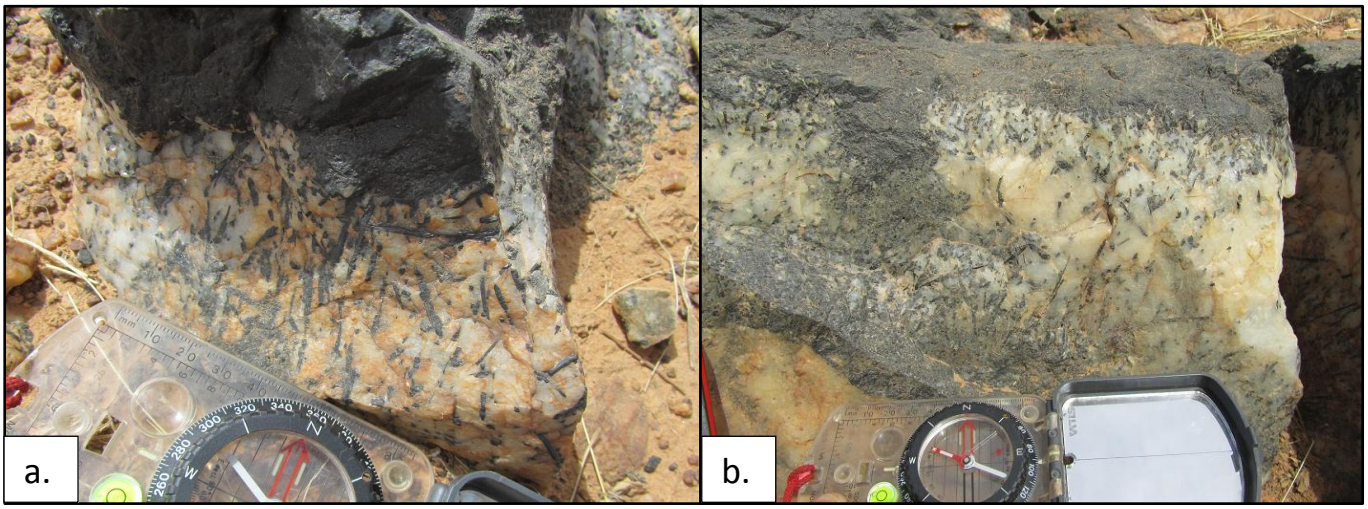

Figure 4.10: Quartz-tourmaline vein with (a) randomly orientated coarse tourmaline crystals and (b) cross-cut by tourmaline veins with crystals radiating out from veins.

5. Petrography

The petrographic study included 16 thin section samples of the Kel Enguef metamorphic belt. These were chosen as representative samples of the stratigraphy. The focus of the petrographic study was on the textural features and mineral assemblages in order to establish the original rock types and the conditions which lead to metamorphism of the metamorphic samples. The study splits the samples into the various facies. Intrusive samples focus on the mineralogy.

5.1 Unit descriptions

Amphibolite

Amphibolite samples consist of fine-grained and equigranular minerals up to 0.3 mm (Fig. 5.1). The amphibolite is dominated by quartz and hornblende, with plagioclase in low concentrations. Mineral proportions of the whole rock are approximately hornblende: 54%; quartz: 40% and plagioclase 6%. The amphibolite is host to a compositional banding texture which is exhibited by the presence of compositional banding. Banding comprises hornblende- and quartz-rich bands. The hornblende rich-bands comprise subhedral crystals of hornblende, 0.2 mm in size and randomly orientated. Quartz inclusions are common in the hornblende crystals. Quartz is typically coarser grained, up to 0.3 mm, with an irregular sub-rounded shape. Plagioclase occurs as an accessory mineral and is subhedral. Plagioclase crystals have fine bladed muscovite inclusions. Quartz compositional bands, up to 1mm in thickness, are characterised by elongated quartz crystals that are orientated parallel to the bands. Hornblende is found in trace amounts and plagioclase is absent. Low strain is exhibited and grain boundary migration is relatively low.

Greenschist

Greenschist facies samples were selected from each of the greenschist sequences from the north and south ridge. They are dominated by quartz crystals with varying amounts of muscovite, iron oxide, epidote and chlorite. The degree of strain is high throughout the sample set.

Samples from the southern ridge exhibit a dominant fabric which is produced by the elongation of crystals, specifically quartz, and the orientation of microcrystalline zones. Two different zones, which are distinguished by grain sizes, are identified in the samples. One

zone consists of medium to fine-grained quartz crystals with minor amounts muscovite. Quartz crystals are irregular in shape and exhibit undulose extinction (Fig. 5.2). Quartz crystals also exhibit intense grain boundary migration between one another. Crystals are elongate parallel to the microcrystalline zones (Fig. 5.2). Fractures, which are occasionally filled with red iron oxide, crosscut the quartz crystals (Fig. 5.2). Rare muscovite is fine-grained. The second zone is composed of microcrystalline quartz (dominant) and muscovite and epidote which vary in size from fine- to medium-grained. The microcrystalline zones are preferentially orientated and range in thickness up to 2 mm. Angular quartz crystals (up to 1 mm in size) occur where these zones are thickest. Where thin, a flow texture is present made up of very fine elongated crystals of quarts and minor muscovite. Epidote, an uncommon mineral, is elongate and up to 1 mm in length. Red opaque iron oxides are common within the zones and are either blocky and clustered where zones are thicker or elongated and bladed where zones are thin. Another feature of thin microcrystalline zones is crack-seal fill where fine elongated quartz crystals as fill are oriented perpendicular to the crack direction. Samples from Unit C three contain quartz crystals up to 2 mm in size which are also elongated. Within the microcrystalline zones, muscovite occurs as both fine bladed crystals and larger crystals up to 2 mm in size. Some of the muscovite crystals are deformed and follow the orientation of the microcrystalline zone. Muscovite most commonly has formed parallel to sub parallel with the orientation of the microcrystalline zone but does also occur to it. Samples from Unit D have quartz crystals up to 5mm in size and are irregular in shape with grain boundary migration present.

The sample set from the northern ridge comprises fine-grained crystals of quartz, muscovite, epidote and red iron oxides and has evidence of high strain. There is a preferential fabric direction which is exhibited by elongated quartz crystals and microcrystalline zones (Fig. 5.2). The quartz crystals are approximately 1 mm in size with the presence of zones of coarser and finer crystals. Quartz crystals contain fine fractures where some of these fractures contain iron oxides in small amounts. Grain boundary migration and undulose extinction is common with quartz crystals. Microcrystalline zones are a prominent feature in the samples. The zones vary in size from less than a millimetre up to 2 mm and align parallel to the elongation in quartz crystals. They comprise very fine-grained quartz, fine needles of muscovite and epidote. The texture within the zones varies from needle like to blocky. Epidote occurs in low concentrations with an irregular shape and is fine-grained. The opaque

mineral is typically euhedral to subhedral and is blocky to elongate. Where it occurs in higher concentration it is commonly blocky and forms clumps of rounded minerals.

Migmatite-gneiss

Granulite samples consist of medium- to fine-grained crystals which do not exhibit any strain. The mineralogy consists of quartz, plagioclase and biotite, which are the dominant minerals, and hornblende, monazite, sphene and magnetite, make up approximately 5 % of the rock. Compositional bands are well defined by the presence or absence of biotite (Fig. 5.3). The biotite-rich bands are fine-grained and biotite is preferentially aligned to the banding direction. Quartz and plagioclase are irregular with the occurrence of grain boundary migration. Quartz-rich bands are medium-grained with crystals up to 2 mm in diameter. Interstitial magnetite, associated with monazite and sphene, is common in these bands and also occurs as inclusions. Quartz is irregular in shape, fractured, and hosts small plagioclase inclusions. Plagioclase is 1 mm or smaller in size and is subhedral. Sericite replacement of plagioclase is common with the presence of fine-grained muscovite on grain boundaries and as inclusions. Biotite is present as an accessory mineral in these zones. Irregular to subhedral grains of monazite and sphene are evenly distributed throughout the rock.

Gabbro

Samples are made up of medium- to fine-grained crystals of plagioclase, actinolite with accessory muscovite, sericite and chlorite in varying amounts depending on the sample. A high degree of alteration is evident due to the textures present. Crystals are undeformed and there is no presence of a well-defined fabric. However minerals are aligned in regions of the thin section. Samples that contain a relatively even distribution of actinolite and plagioclase (Fig. 5.4) consist of actinolite ranging in size from medium- to fine-grained. Medium-grained crystals are elongated and subhedral whereas fine-grained crystals are irregular. Quartz and plagioclase inclusions are typical in actinolite. Plagioclase crystals are irregular in shape and range from medium- to fine-grained. Levels of alteration vary throughout the sample. Relatively unaltered plagioclase crystals are present with minor sericite. Altered plagioclase crystals are almost completely recrystallised in the form of sericite, muscovite and fine grained cloudy minerals. Remnant twinning is present in these altered plagioclase crystals. The abundance of actinolite and plagioclase vary in samples. Actinolite may also be dominant (85 %) with an absence of plagioclase. These samples comprise coarse-grained

actinolite which is aligned in parts of the sample. Chlorite is present (8 %) in this sample with accessory muscovite, sericite and quartz.

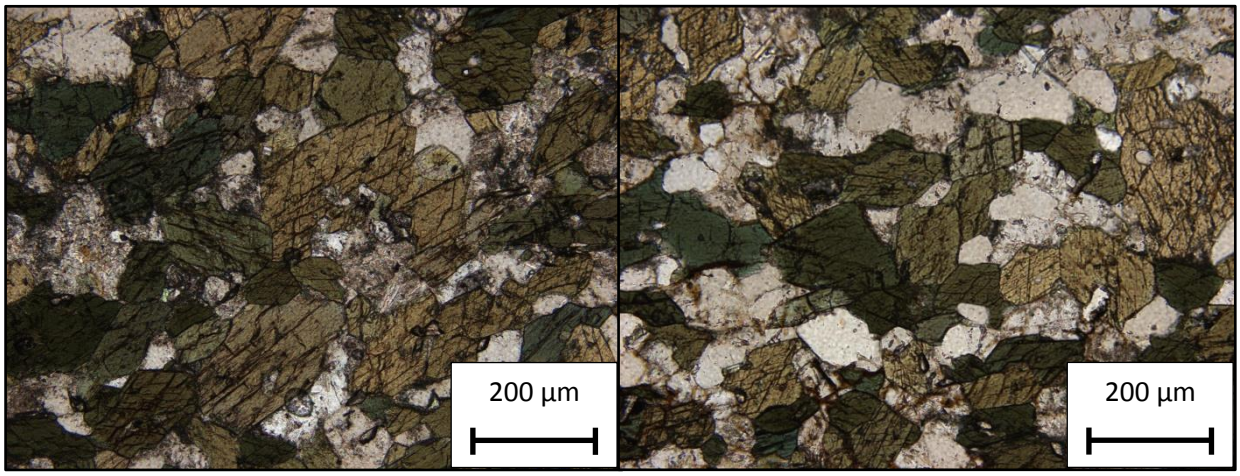

Figure 5.1: Amphibolite with randomly orientated, subhedral hornblende and quartz crystals

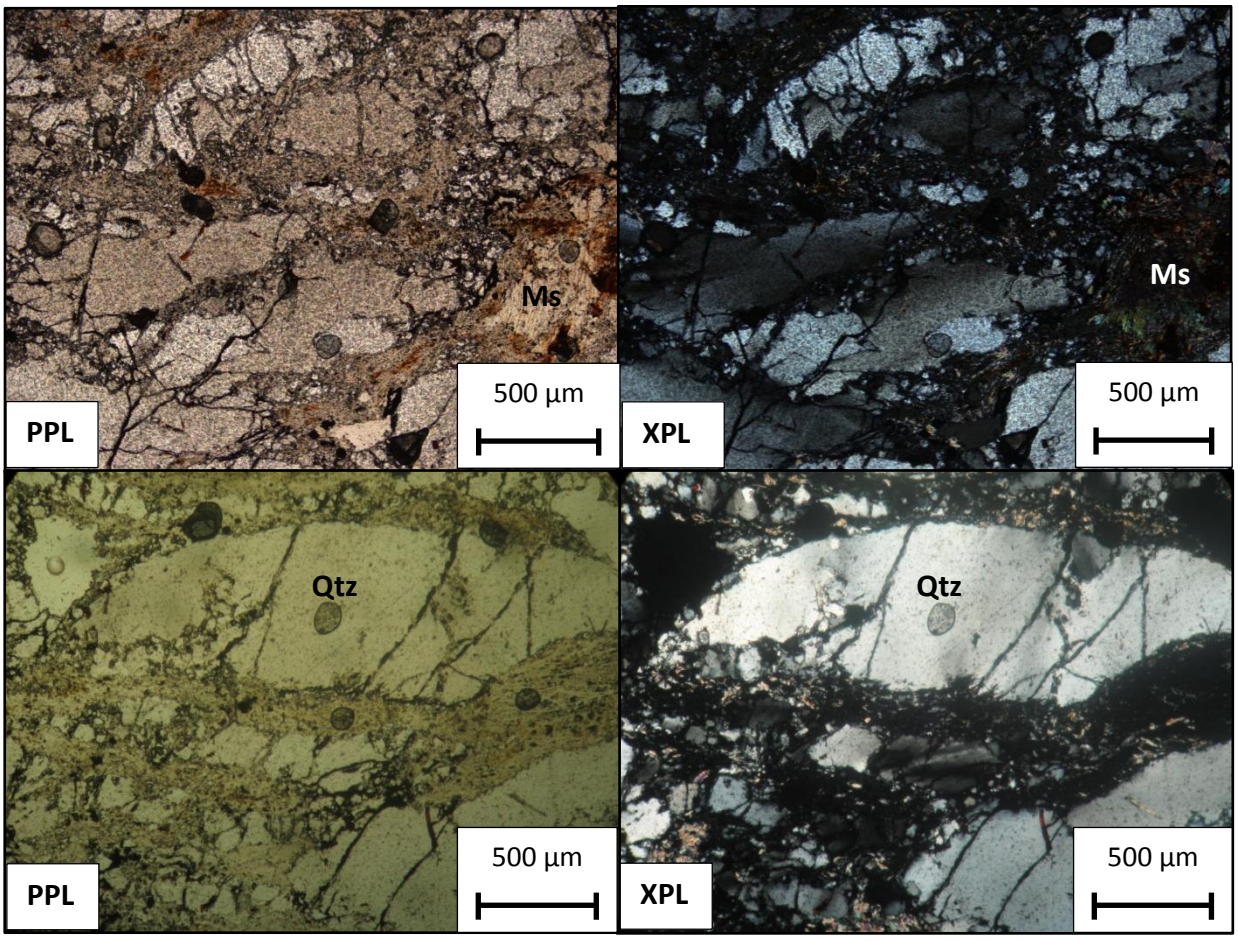

Figure 5.2: Greenschist facies rocks with medium-grained, elongated quartz crystals which are fractured and microcrystalline zones of quartz (Qtz), epidote and muscovite forming the foliation with larger muscovite (Ms) crystals within.

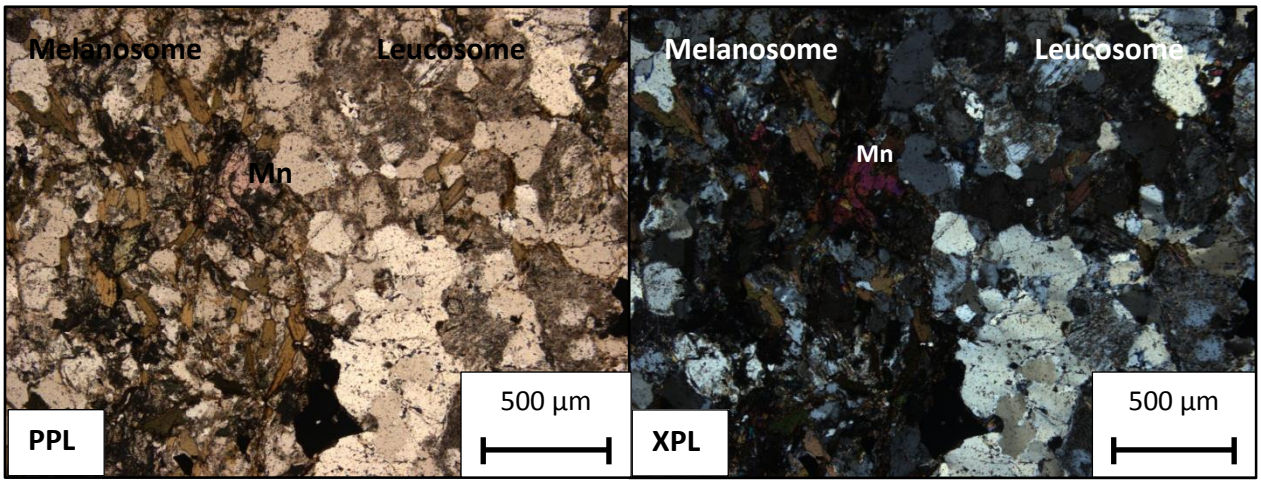

Figure 5.3: Migmatite with melanosome (biotite-rich) and leucosome (quartz-plagioclase-rich) zones and monazite (Mn) crystals

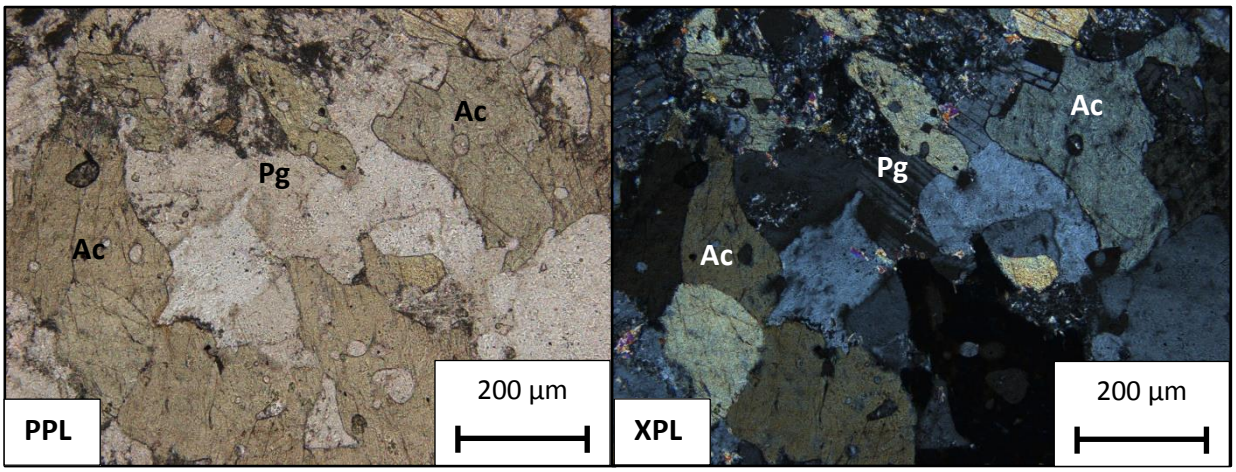

Figure 5.4: Metamorphosed gabbro with actinolite (Ac) and altered plagioclase (Pg)

Diorite

Diorite samples comprise quartz, plagioclase and minor biotite and muscovite in small amounts. Quartz and plagioclase are equigranular which are undeformed. There is a homogenous distribution of minerals with no fabric or deformation present. Quartz crystals are irregular with jagged grain crystal boundaries and are 1 to 3 mm in size. Grain boundary migration is relatively low. Quartz exhibits undulated extinction. Plagioclase and small bladed biotite inclusions are present. Plagioclase crystals are subhedral and up to 1 mm in size. There is replacement of plagioclase by muscovite on grain boundaries, irregular and up to 2 mm in size, and fine inclusions within plagioclase. Biotite is fine grained, interstitial and makes up about 1 % of the rock. Quartz and plagioclase are present at 60 % and 35 % respectively. Muscovite makes up 5 % of the rock.

5.2 Overview

The rocks of the KEMB exhibit varying degrees of deformation and metamorphic grades. In summary, the amphibolite comprises a fine-grained mineral assemblage of hornblende, quartz and plagioclase. Hornblende and quartz are the dominant minerals and plagioclase occurs in low concentrations. Compositional banding is present in the rock and produces hornblende-rich and quartz-rich zones. The minerals do not align with these zones and rather have a granoblastic texture. The greenschist rocks are highly deformed and poses a strong fabric. A mineral assemblage of quartz-muscovite ±epidote ±chlorite makes up the rock. Quartz is the dominant mineral (>90%) and ranges in size from fine- to coarse-grained in the various samples. The quartz crystals are elongated in a preferential direction which is parallel to microcrystalline zones which are a typical feature of the greenschist rocks. Within the microcrystalline zones, minerals such as muscovite, iron oxides, epidote and chlorite are present. The zones vary in thickness and are pervasive throughout the rock. The migmatite has a mineral assemblage of quartz-plagioclase-biotite-magnetite-monazite-sphene. Compositional banding is dominant feature of the migmatite with the separation of minerals into leucosome (quartz-plagioclase-magnetite-monazite-sphene) and melanosome (biotite-dominant) bands. Biotite is elongated parallel to the compositional bands. The meta-gabbro dykes comprise the mineral assemblage actinolite-plagioclase-chlorite-sericite-muscovite. Crystals range in size from medium- to fine-grained with course-grained actinolite in parts. The mineral are irregular in shape and inclusions and replacement minerals are a common feature in actinolite and plagioclase respectively. A fabric is not present in the samples. The

diorite has an equigranular texture comprising a mineral assemblage of quart-plagioclase-biotite-muscovite. Samples do not indicate deformation and the rock is relatively unaltered.

6. Mineralogical study

6.1 XRD data

Two samples (samples A & B) of the iron stone out crop were analysed by XRD. An interpretation of the diffractograms indicates the presence of magnetite, hematite, goethite and cassiterite (Fig. 6.1). Therefore there is the presence of iron and tin in the samples.

6.2 Ore block study

The study of the samples indicates an abundance of magnetite and hematite. Fractures are a dominant feature of the samples (Fig. 6.2a). The two minerals occur in close association with one another. The composition is approximately 60 % magnetite and 40 % hematite. Magnetite occurs as fine fragments with straight regular edges surrounded by hematite (Fig. 6.2b). This textural relationship of the minerals indicates hematite is replacing magnetite. The hematite extends out from the fine fractures. In some parts magnetite is found in low amounts where it has almost been completely replaced. Cassiterite was not seen in the ore blocks.

Samples of the iron-rich quartzite indicate a similar occurrence of magnetite and hematite. Due to the interstitial nature of the Fe-rich minerals (Fig. 6.3a & 6.3b), it has been determined that the minerals are secondary, possibly utilizing pore spaces. Hematite replaces magnetite in a very similar manner to the above example (Fig. 6.3c & 6.3d) where is propagates out from fractures.

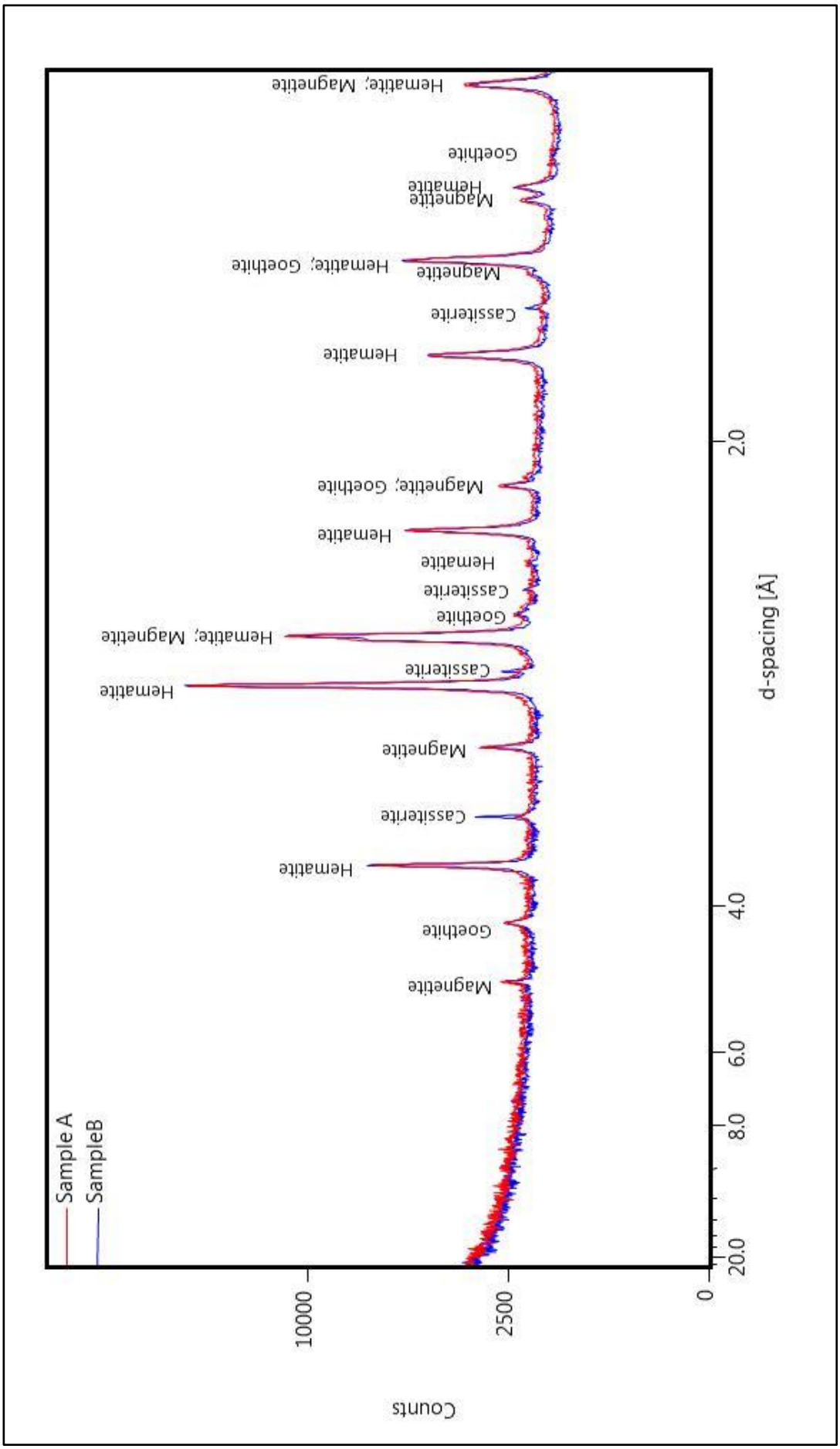

Figure 6.1: Diffractograms from XRD scan of two iron stone samples.

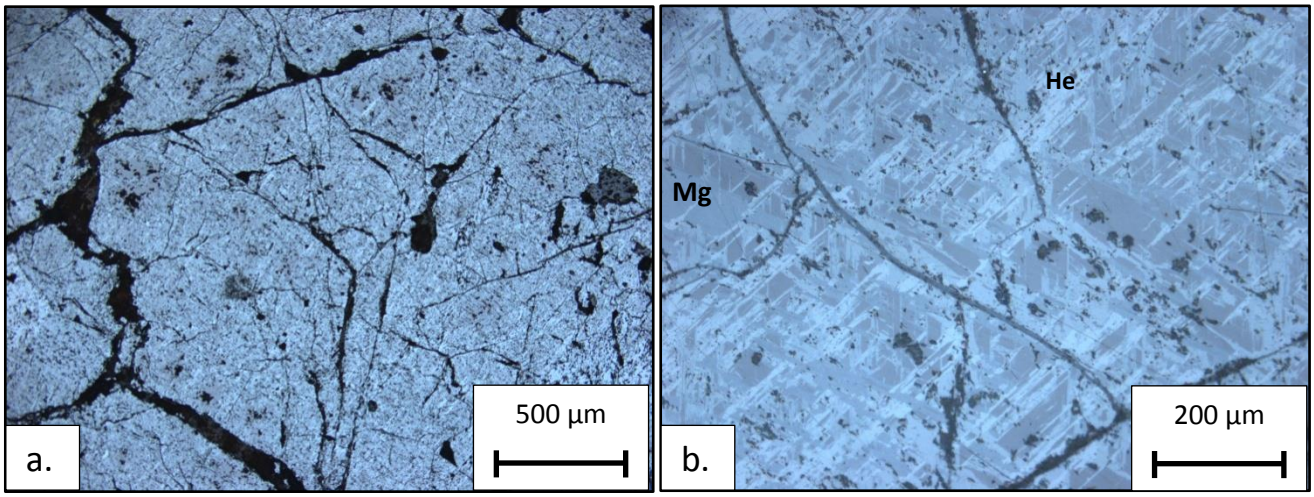

Figure 6.2: Iron stone ore blocks in reflective light. a) highly fractured rock. b) hematite (light mineral-He) replacing magnetite (dark mineral- Mg).

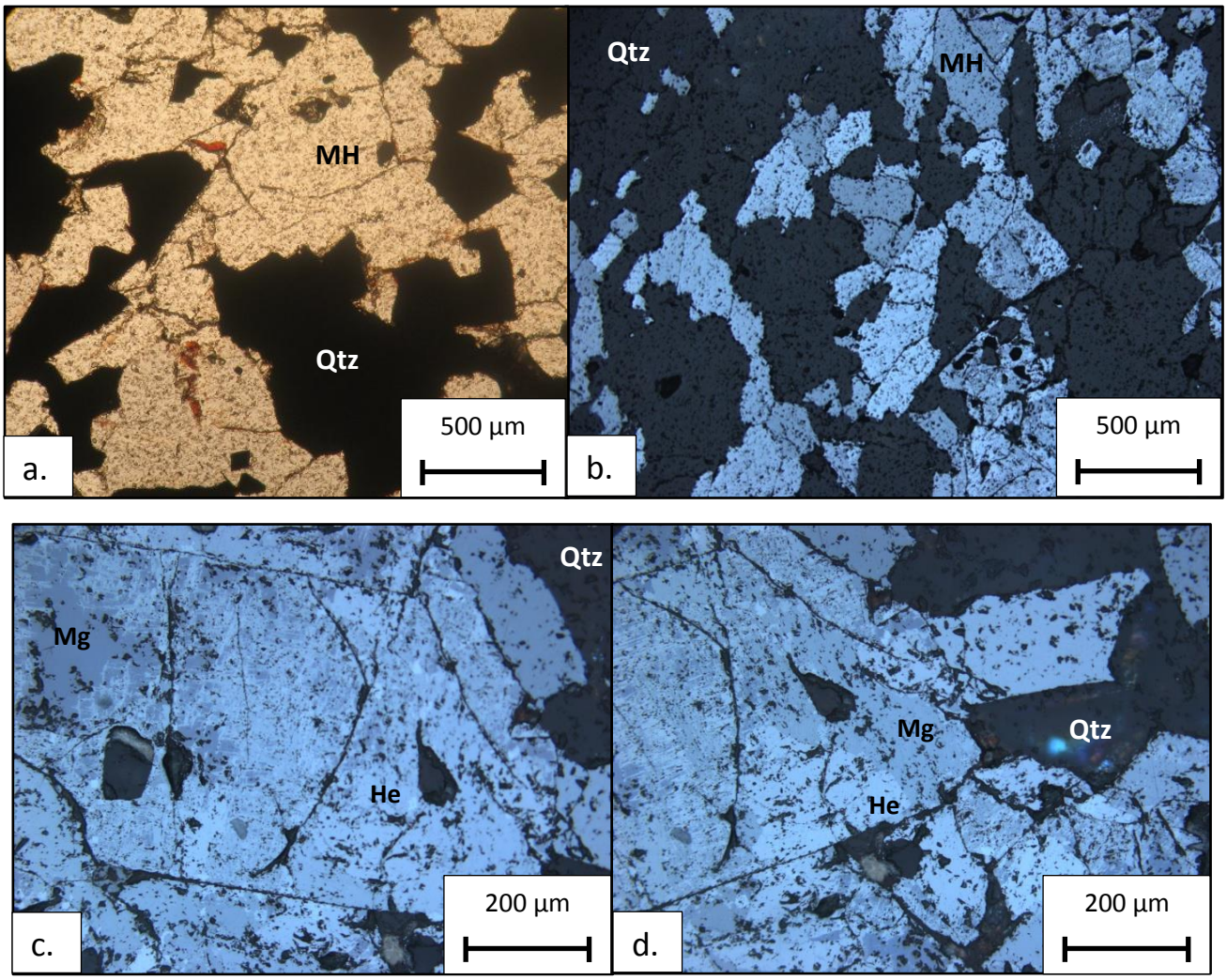

Figure 6.3: Ferruginous quartzite. a) transmitted light through thin section showing quartz crystals (light mineral-Qtz) and interstitial magnetite and hematite (black mineral-MH). b) reflective light of ferruginous quartzite. c & d) fractures crystals with hematite replacement (light mineral-He) of magnetite (dark mineral-Mg).

7. Interpretation and discussion

7.1 Protolith and depositional environment

The metamorphosed sequences of the KEMB have been subjected to high stress and a range of temperatures which is evident by the cleavage and metamorphic facies present. The mineralogy of the metamorphosed rocks and the preservation of bedding are indicative of a sedimentary protolith. The metamorphosed rock is quartz dominated with a composition of more than 90 % quartz. Other minerals present are muscovite, epidote, chlorite, hornblende and iron oxide. Bedding is dominantly planar, with cross-bedding features apparently absent, and ranges in thickness from a few centimetres to several metres. Within bedding, grain-size is typically uniform, with no upward- fining or coarsening trend. The absence of typical sedimentary features such as cross-bedding and graded bedding may be attributed to the high degree of strain accommodated by the rocks. In the east of the northern ridge units, the scattered hillocks of coarser units surrounded by the low lying finer units possibly indicate lateral facies changes.

The high silica content, in the form of quartz crystals and microcrystalline quartz, suggest a sandstone protolith. This is consistent with the metamorphic mineral assemblage of quartz-muscovite-iron oxide± chlorite± epidote (Nesse, 2000). A dominant feature throughout the greenschist rocks is the anastomosing, microcrystalline zones which occur in thin section as dark bands with varying thickness (Fig. 5.2). A possible explanation for the microcrystalline zones is the formation of a fracture cleavage which utilises the less competent matrix (Spry, 1969). Although no matrix is observed in thin section, the pervasive nature, varying thickness and the way the microcrystalline zones anastomose around quartz crystals suggests the deformation of finer material (matrix) which was once present. Thin sections reveal that these microcrystalline zones make up 10 to 30 % of the rock depending on the sample and where in the stratigraphy it is located. This indicates that the rock originally comprised up to 30 % matrix. However, volume reduction should also be considered if the stress applied on the rocks was great. The protolith would therefore have been a quartzwacke (Fig. 7.1) based on the amount of matrix once present and the absence of lithic fragments and feldspathic grains (Boggs, 2006).

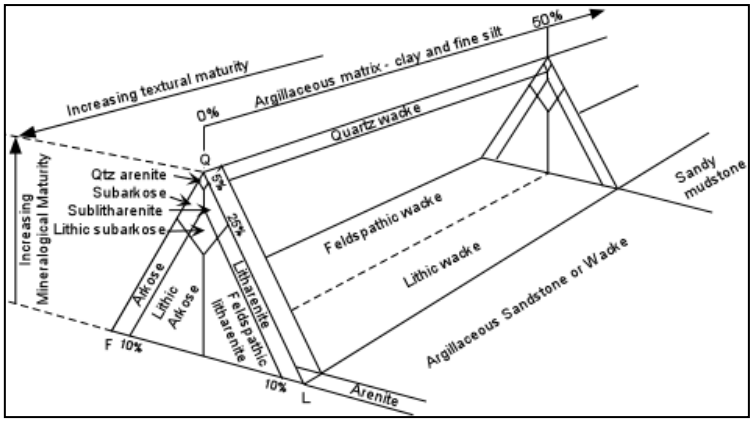

Figure 7.1: Classification of sandstone (Boggs, 2006)

The KEMB is split into three clastic sedimentary metamorphic units, namely the northern ridge, southern ridge and southern region units. These three units comprise one or more successions with ranging grain size. The southern region (amphibolite) unit comprises a fine-grained succession. The dominant metamorphic overprint has destroyed all evidence of sedimentary features such as bedding and grading sequences. Stratigraphically above this is a banded ironstone formation (BIF) that consists of interbedded shale and iron precipitate. In turn stratigraphically above the BIF, the southern ridge units comprise medium- to fine-grained quartzite (Units A & B), overlain by a medium-grained quartzite (Unit C) grading up to a coarse-grained quartzite (Unit D). Overall, there is an increase in grain size over a thickness of approximately 150 m. The northern ridge units comprise a fine- to medium-grained quartzite (Units X & Z) with a coarse, pebble like interbed (Unit Y). The eastern side of the northern ridge is host to facies changes, of high and low energy. Here coarser sequences are located a largely predominant fine-grained sequence.

Due to the greenschist facies rocks having more sedimentary features preserved relative to the amphibolite rocks, they are more useful in determining the depositional environment. Considering the protolith of quartzwacke, which is extensive and occurs in beds up to a metre or more thick as well as the coarsening upward sequence in the southern ridge and pebble like nature of Unit Y between Units X & Z of the northern ridge, a deltaic depositional environment is interpreted (Reading, 1978). The overall upward coarsening trend of the southern ridge is indicative of a progradational deltaic sequence (Reading, 1978; Leeder, 1999). However, typical channel forms and shapes, expected in a deltaic environments (Reading, 1978) are absent. In general, the fine sequences are representative of the distal bar to prodelta setting (Leeder, 1999 and Nichols, 2009). The medium-grained sequences are

representative of the sandy distal mouth bar while the coarse-grained sequences are representative of a gravelly proximal mouth bar to sandy distal mouth bar of a typical delta (Nichols, 2009). The interlamination of sands and silts will occur between the sandy distal bar mouth bar and the prodelta (Fig. 7.2).

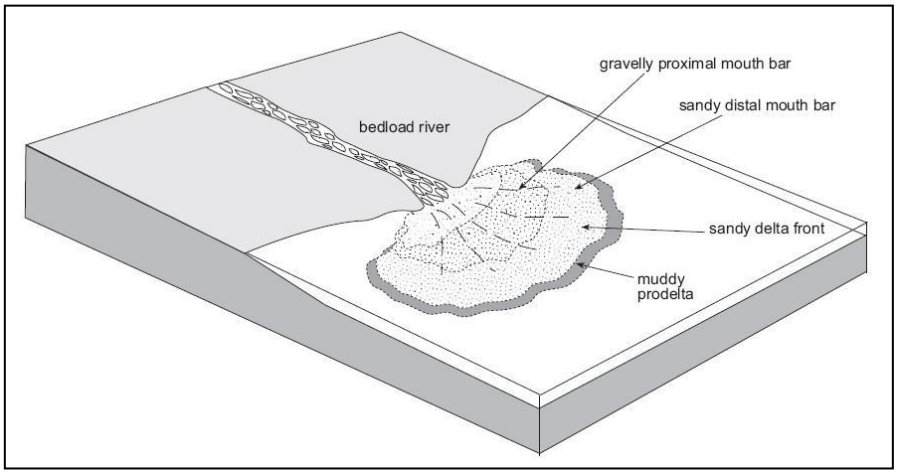

Figure 7.2: Coarse-grained delta (Nichols, 2009)

Interpreting the sequences present in the greenschist ridges, a prograding delta would account for the overall upward coarsening profile (Fig. 7.2). The sequences in the northern ridge suggest progradation from a medium-grained to a course-grained/pebble sequence, followed by retrogradation to a medium-grained facies sequence. The deltaic environment determined from the metaclastic succession allows for the interpretation of the underlying banded iron-formation and amphibolite. Although definitive evidence of a conformable contact between the iron-formation and the metaclastics was not observed, the increase in metamorphic grade and facing direction suggests that these sequences occur lower in the stratigraphy. The occurrence of the banded ironstone formation is typical of shallow water environments of the Proterozoic (Leeder, 1999). This would have occurred distal to a delta setting on a shelf or proximal to the delta during periods of reduced sedimentation. The fine-grained sediment of the amphibolite would have been deposited in the prodelta in the form of shales or mudstone.

The described protoliths of quartzwacke, shale and possible pebble quartz arenite fit well with the sedimentary rocks of the Birimian Supergroup and in particular the Oudalan-Gorouol greenstone belt described by Pons et al., 1995; Debat et al., 2003; Tshibubudze et al., 2009; Tshibubudze and Hein, submitted. Therefore the sequences described may represent a portion of the Oudalan-Gorouol greenstone belt and this would also be enforced by the KEMB close proximity to the belt, to east of the Markoye shear zone,

7.2 Metamorphic history

The overall metamorphism of the KEMB increases very rapidly in grade from greenschist facies in the north to amphibolite facies in the south. The mineral assemblage of the greenschist grade rocks are quartz-muscovite-iron oxide ± epidote ± chlorite. Pressure-temperature conditions specific to this assemblage are between 2 to 4 kbar at temperatures of 250 to 450^{0}C (Nesse, 2000). The amphibolite has the general mineral assemblage of quartz-hornblende-plagioclase. This assemblage is typical of conditions of 2 to 5 kbar at temperature of 450 to 650 ^{0}C (Nesse, 2000). These conditions are satisfied by a normal geothermal gradient (Fig. 7.3). Thus subsidence and burial to suitable depth, by some or other process, would have resulted in the formation in the facies observed by regional metamorphism.

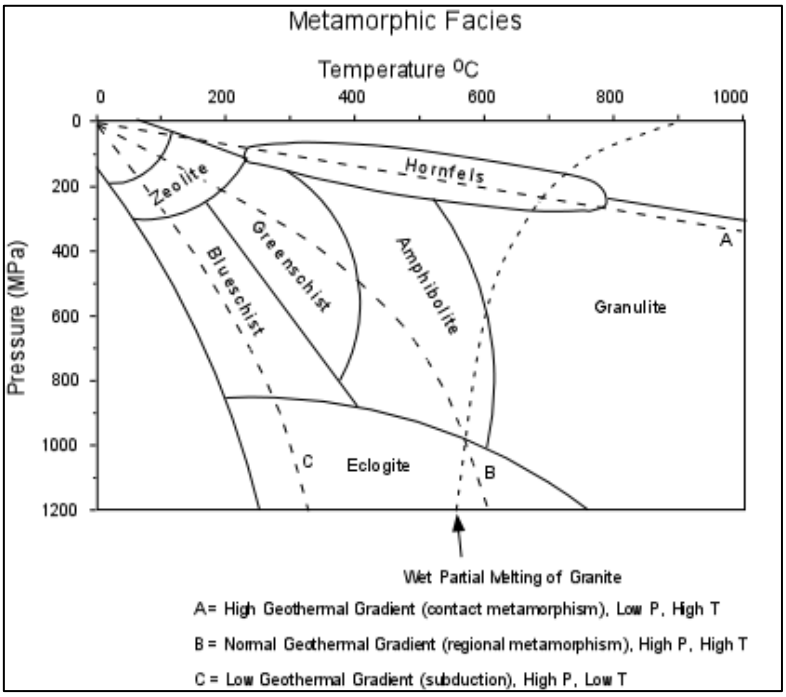

Figure 7.3: Metamorphic facies and geothermal gradients (Nelson, 2003)

Features within the metamorphic rock assist in determining how metamorphism occurred. The greenschist contains bedding parallel foliation which is defined by the elongation and alignment of quartz crystals and microcrystalline anastomosing zones, possibly representative of where pressure solution may have also occurred. Deformation to crystals appears to be axial which is indicated by the absence of shearing and rotation of crystals. Undulose extinction, grain elongation defining a foliation and recrystallisation, all exhibited by quartz crystals, are produced at low to moderate temperatures and pressures (Vernon, 1976; Vernon & Clarke, 2008). This is what is expected in greenschist facies. Under experimental

conditions, using axial compression, intragranular recrystallisation can be achieved at temperatures of 300 to 400 ^{0}C with confining pressures of 10 to 15 kbar in the presence of structural hydroxide (Vernon, 1976). A part from the elongated quartz crystals, strain is largely contained within the matrix surrounding the grains in the quartz wacke (Spry, 1969). Deformation has formed a foliation in the rock which is described as closely spaced, irregular zones which anastomose around fragments of clastic grains (Fig. 16), namely quartz. The formation of the foliation and grain elongation would have occurred resulting in volume loss under compression. This foliation is sub-parallel to the bedding plane. Bedding parallel foliation is commonly associated with shales that have been subjected to low stress during burial under normal diagenetic processes (Vernon and Clarke, 2008). However, bedding parallel foliation in the metamorphosed rocks of the KEMB is in quartz wackes that have reached much greater depths as indicated by the greenschist facies mineral assemblage.

The amphibolite comprises quartz and hornblende which are subhedral. The unit contains prominent compositional banding of quartz-hornblende and quartz. Hornblende crystals are not preferentially orientated parallel to the compositional banding (Fig. 15). The compositional banding may represent either original depositional features, strain induced banding forming a foliation or quartz veining that has been deformed. Quartz veining would be unlikely as the compositional banding is pervasive, fine and relatively regular. It would be highly unlikely for quartz veins to cut through the rock at such regular intervals to form what is observed as banding. The possibility of the banding representing bedding features of the original rock is something to consider however this will be difficult to prove. Considering what is seen in the above greenschist rocks which contain a strong fabric, it is interpreted that this compositional banding was also induced from stress related to the formation of the greenschist foliation. The formation of isoclinal folds in the unit, with fold hinges parallel to foliation, formed during high compaction accommodation volume loss (Davis and Reynolds, 1996).

Previous studies of the metamorphism in the WAC concluded regional metamorphism to greenschist facies occurred during crustal shortening of the Eburnean Orogeny (Vidal et al, 1996; Beziat et al., 2000; Debat et al., 2003; Hein et al., 2004; Naba et al., 2004). Metamorphism to amphibolite facies was concluded to occurred during contact metamorphism by the emplacements of the various plutons (Pons et al., 1995; Debat et al., 2003; Tshibubudze et al., 2009) However a more recent study in the Oudalan-Gorouol

greenstone belt concluded amphibolite facies was reached during regional deformation (Tshibubudze and Hein, submitted).

To explain the metamorphic grade and deformation exhibited by the rocks of the KEMB, the following possibilities are proposed.

1. The rocks were deformed and metamorphosed during regional deformation events as proposed by Tshibubudze and Hein (submitted). Attaining bedding-parallel foliation would be difficult to achieve unless the rocks were orientated at a high angle to the primary stress direction. This would have occurred either during SW directed shortening of the Tangaean Event or SE-NW shortening of the Eburnean Orogeny (Tshibubudze et al., 2009; Hein 2010; Tshibubudze and Hein, submitted). This would have a required the units to be forced into a steep orientation prior to one of the events. Following deformation, the units would then require subsidence and tilting.
2. Burial to depths of approximately 10 to 12 km. Subsequent metamorphism and deformation would be expected due to the geothermal gradient as well as a large amount of force exerted by the overlying rocks which would result in compaction. Producing bedding-parallel foliation would be challenging by such a process as it would require the descent of rocks to a great depth remaining in the same position as they were deposited in. However bedding-parallel foliation as well as isoclinal fold hinges parallel to the bedding plane is strong evidence for this type of deformation. Thus it is suggested that crustal extension following deposition resulted in the subsidence and burial of the rocks of the KEMB. Thinning of the crust as well as a higher geothermal gradient prosed for the Precambrian would have resulted in subsequent metamorphism.
3. Contact metamorphism related to the emplacement of a pluton. This has been proposed by Pons et al. (1995), Tshibubudze et al. (2009) and Tshibubudze and Hein, (submitted). However, this does not explain the presence of the foliation and therefore is not the favoured explanation.

Regional deformation or burial metamorphism could explain the formation of foliation. However it is evident that the rocks of the KEMB did reach crustal levels great enough to achieve amphibolite facies and form compositional banding within the amphibolite rock.

7.3 Migmatite formation

A migmatite results from the partial melting of a pre-existing rock. The formation of migmatites is generally associated with an increase in pressure and temperature as either an increase in depth, known as “static melting”, or an increase in differential stress, known as “dynamic melting” (Ashworth, 1985 and Sawyer, 2008). In the absence of free fluid, melting reactions occur at granulite facies conditions, typically at temperature between 800 to 1000 ^{0}C (Vernon and Clarke, 2008).

However the occurrence of the migmatite in the KEMB is not associated with a typical increase in temperature and pressure along a geothermal as described above. This is due to its anomalous position between greenschist and amphibolite facies. Outcrop suggest the migmatite has little lateral extent and is isolated to an area of only several hundred metres. The closest occurring migmatite in the surrounding area is situated approximately 20 km away on the northern margin of the Dori Batholith and is interpreted as the product of aureole deformation during the emplacement of the batholith (Tshibubudze and Hein, submitted). However aureole deformation is not indicated in the KEMB as there is no intrusion in contact with the migmatite.

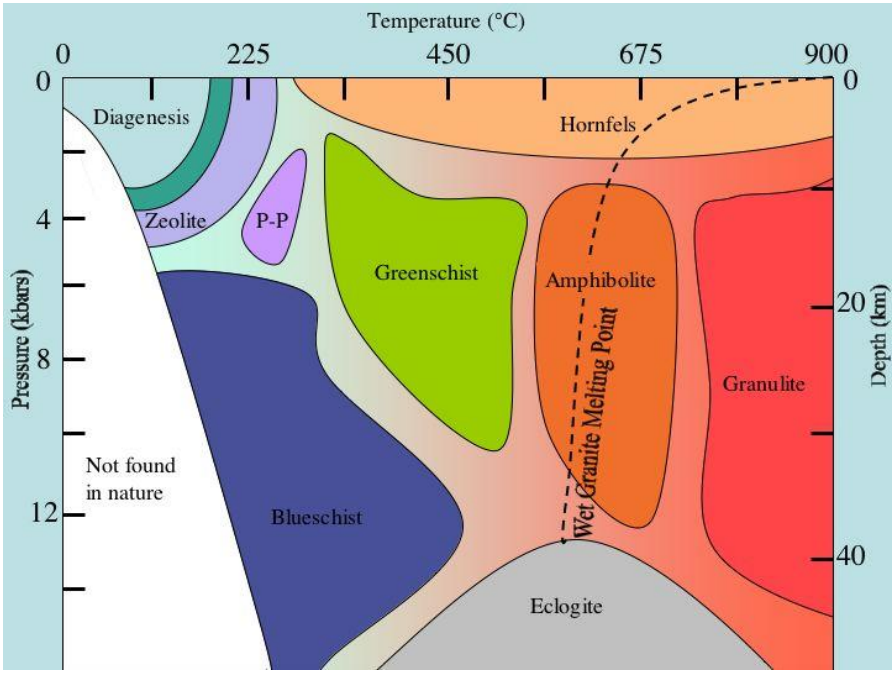

Figure 7.4: Diagram indicating the melting temperature of wet granite (David Magrass and Brian Wells, 2010)

Another process by which a migmatite can form is during metasomatism (Sawyer, 2008). The presence of fluids is known to act as a flux and thus can reduce the melting temperature (Fig. 7.4) by changing the solidus (Ashworth, 1985;Sawyer, 2008; Vernon and Clarke, 2008).

Fluid interaction, to induce melting, can take place in two ways:

1. Metasomatism before melting (Sawyer, 2008). The infiltration of metasomatic fluids from an outside source involves the enrichment of the rock by improving the rock fertility (Vernon and Clarke, 2008) thus making it more susceptible to melting. This involves hydrothermal alteration and the production of new minerals**.** The amount of water in the fluids leads towards the second type of fluid interaction.
2. Introduction of hydrous fluids from an external source known as H_2O-saturated melting (Ashworth, 1985; Sawyer, 2008; Vernon and Clarke, 2008). The presence of water as well as other compounds (such as P_2O_5, HF, LiOH) can drastically reduce the solidus temperature (Ashworth, 1985).

Furthermore, the dehydration of hydrous minerals under high pressures releases water into the rock and induces melting (Vernon and Clarke, 2008). Considering the KEMB and related pressure-temperature conditions, would it have been possible to produce a migmatite? The migmatite is situated between the greenschist and amphibolite facies. Here temperatures would have been in excess of 450 ^{0}C (c.f., Vernon and Clarke, 2008). The influx of fluids at these temperatures would not have been sufficient to induce melting. However there is the presence of several large plutons in the surrounding area which include the Tin Taradat granodiorite-tonalite, Dori batholith and the Granite Adamelite (Tshibubudze and Hein, submitted). These could have been the source of high temperature igneous related fluids which would have infiltrated the surrounding rocks. These zones of infiltration would have had to be concentrated and localised. The rapid increase of temperature in pre-existing hot conditions could have induced partial melting and dehydration of the rock. Migmatites from Saint-Malo, France, with a very similar mineral assemblage of muscovite-plagioclase-quartz leucosome and biotite-rich melanosome, are interpreted to have formed by the breakdown of muscovite (Sawyer, 2008). Although the Saint-Malo migmatites have been proposed to have formed in upper amphibolite facies, the presence of muscovite in the metamorphosed rock which formed the migmatite in KEMB would have been a source for more hydrous fluid.

Another possibility is that the migmatites are bounded by shear zones and that fluids travelled along the structures and caused the partial melting.

The occurrence of the KEMB migmatite is anomalous and somewhat challenging to interpret. However it can be summarised as a location of partial melting at granulite facies. The most suitable explanation for its occurrence is the influx of high temperature fluid from an external source, either from one of the plutons in the surrounding area or along strictures along the margins of the migmatite. Associated with this was dehydration metamorphism and reactions. Why this occurred here, is the focus of future research studies in the region.

7.4 Tectonic History

The KEMB is host to metamorphosed sedimentary sequences and igneous intrusions. The terrain has been subjected to a series of regional tectonic events. The studies of Tshibubudze et al. (2009) and Tshibubudze and Hein (submitted) have indicated that the KEMB lies west of the Markoye Shear Zone which developed by at least two regional deformation events. Understanding the tectonic history of the KEMB is beyond the scope of this project however based on the metamorphic and structural data collected, a simplified tectonic history can be suggested. Saying this, further studies will be crucial in acquiring a greater understanding of how the KEMB fits in with the regional geology.

The series of metamorphosed sedimentary units have reached metamorphic grades of greenschist and amphibolite facies. An anomalous occurrence of a localised migmatite, which has reached granulite facies, lies between the greenschist and amphibolite and adds complexity to the metamorphic belt. The metamorphosed sedimentary units are separated by areas of sand cover with little outcrop. Later intrusive phases are a feature of the KEMB with the presence of gabbro dykes cross-cutting the central region as well as the occurrence of a diorite pluton.

The tectonic history of the KEMB is summarized below.

1. The deposition of the sedimentary units in a shallow marine, deltaic setting following the formation of a basin. The units include (amphibolite) a siltstone sequence, a BIF sequence, (Unit A) a sandstone sequence, (Unit B) an interbedded siltstone and sandstone sequence, (Unit C) a sandstone sequence, (Unit D) a coarse-grained sandstone sequence, (Unit X) an interbedded siltstone sequence, (Unit Y) a course-grained sandstone and (Unit Z) an interbedded siltstone and sandstone sequence.

2. Burial of the sedimentary units was accompanied by compaction and metamorphism. Burial occurred to a depth of several kilometres as determined by the metamorphic facies reached. The immense overlying weight would have exerted a great stress on the rocks at such a depth, thus resulting in a pervasive bedding-parallel foliation (S_1) and crystal lineation (L_1).
3. Folding (F_2) of the southwest units. The amphibolite, banded ironstone and southern ridge are host to a fold. F_2 is defined in the amphibolite and banded ironstone in the south-eastern region. S_1 is folded about F_2.
4. Intrusion of gabbro dykes prior or during metamorphism of the metaclastic rocks. A petrology study on the dykes determined that there is an abundance of actinolite/tremolite present and an absence of pyroxene. Plagioclase crystals are commonly altered to sericite. The presence of actinolite and altered plagioclase to sericite suggest metamorphism to greenschist facies. Thus the dykes had to be intruded at depth in order to be metamorphosed it such facies.
5. Uplift and tilting of the metamorphosed sedimentary units and dykes to the north indicated by the dip of bedding-parallel foliation.
6. The intrusion of the diorite pluton. There are several granodiorite plutons that occur in the surrounding area (Tshibubudze and Hein, submitted). The most likely source of the pluton in KEMB could be a younger batholith related diorite intrusions south of the town of Gorom Gorom.
7. The formation of the ferricrete horizons followed by the tertiary sands. Ferricrete horizons in the WAC formed during the Cretaceous and associated with the development of in situ laterite (Brown et al., 1994; Burke and Gunnell, 2008).

Suggestions tectonic uplift is proposed due to the result of either one of two events. The emplacement of the Dori Batholith, preceding the Tangaean Event (Tshibubudze and Hein, submitted), to the southeast of the field area may have resulted in the uplift and tilting of the KEMB. This would have been due to the crust being pushed out and up to accommodate the large volume of magma being emplaced beneath. The northerly dipping bedding-parallel foliation of the metamorphosed units in the KEMB would agree with this. Another proposed event is the NW-SE crustal shortening of the Eburnean Orogeny (Tshibubudze et al., 2009 and Tshibubudze and Hein, submitted) which may also have resulted in the uplift and tilting

of the KEMB. The NW compression and resulting thrusting could have caused tilling of the stratigraphy to the north exposing deeper crustal levels.

8. Conclusions

The deformation and metamorphism present in the KEMB is complex and not easily explained. This can be linked to the series of tectonic events which have occurred in the region and the terrain that the KEMB exists in. In light of this, far more is now known about the KEMB and the outcomes of this project can lead to further work in understanding how the KEMB fits in with the regional geology.

The following conclusions are drawn about the KEMB. The rocks comprise metamorphosed sedimentary and intrusive rocks. The deposition of the sedimentary sequences occurred in a deltaic environment into a shallow marine setting. These rocks were subsequently buried to an estimated deep crustal level where the associated pressures and temperatures metamorphosed the rocks to greenschist and amphibolite facies. The result of either compaction associated with the weight of the overlying rock and crustal shortening during the regional deformation events formed a strong foliation in the sedimentary sequences. The intrusion of gabbro dykes and a diorite pluton occurred after such events. The tectonic uplift and tilting of the rocks was followed by erosion and the formation of ferricrete horizons leading to the exposer of the rocks as seen today.

The presence of an iron stone and ferruginous quartzite as well as quartz-tourmaline veins indicates the potential for economic deposits. The surface extent of these outcrops do not suggest a great extent of the mineralisation. However the sign of such occurrences do raise interest for further research into possible large deposits of such kinds.

9. Acknowledgments

The author would like to thank WAXI (West African Exploration Initiative), the Amira Group and its sponsors, Asinne Tshibubudze for his guidance and Prof. K.A.A Ncube-Hein for her supervising, guidance and the overseeing of this project.

Sponsors and research partners of the Amira Group:

10. References

Béziat, D., Bourges, F., Debat, P., Lompo, M., Martin, F., Tollon, F., 2000. A Paleoproterozoic ultramafic-mafic assemblage and associated volcanic rocks of the Boromo greenstone belt: fractionates originating from island-arc volcanic activity in the West African craton. Precambrian Research, **101**, 25-47.

Boggs, S., 2006. Principles of sedimentology and stratigraphy, 4th Edition, Pearson Prentince Hall. 662p.

Castaing, C., Billa, M., Milesi, J.P., Thiéblemont, D., Le Metour, J., Egal, E., Donzeau, M., Guerrot, C., Cocherie, A., Chevremont, P., Tegyey, M., Itard, Y., Zida, B., Ouedraogo, I., Koté, S., Kabore, E., Ouedraogo, C., Ki, J.C., Zunino, C., 2003. Notice explicative de la carte géologique et minière du Burkina Faso à 1/1 000 000., Orléans: Edition BRGM-3. Avenue C. Guillemin-BP 6009-45060-Orleans Cedex 2-France: (2) Bumigeb-01 BP601 Ouagadougou 01- Burkina Faso.

Davis, D. W., Hirdes, W., Schaltegger, Nunoo, A., 1994. U–Pb age constraints on deposition and provenance of Birimian and gold-bearing Tarkwaian sediments in Ghana, West Africa. Precambrian Research, **67**, 89-107.

Debat, P., Nikiéma, S., Mercier, A., Lompo, M., Béziat, D., Bourges, F., Roddaz, M., Salvi, S., Tollon, F., Wenmenga, U., 2003. A new metamorphic constraint for the Eburnean orogeny from Paleoproterozoic formations of the Man shield (Aribinda and Tampelga countries, Burkina Faso). Precambrian Research, **123**, 47-65.

Feybesse, J.-L., Billa, M., Guerrot, C., Duguey, E., Lescuyer, J.-L., Milesi, J.-P., Bouchot, V., 2006. The paleoproterozoic Ghanian province: geodynamic model and ore controls, including regional stress modelling. Precambrian Research, **149**, 149-196.

Hein, K.A.A, Morel, V., Kagone, O., Kiemde, F., Mayes, K., 2004. Mirimian lithological succession and structural evolution in the Goren segment of the Boromo-Goren Greenstone Belt, Burkina Faso. Journal of African Earth Sciences, **39**, 1-23.

Hein, K. A. A., 2010. Succession of structural events in the Goren greenstone belt (Burkina Faso): Implications for West African tectonics. Journal of African Earth Sciences, **56**, 83-94.

Hirdes, W., Davis, D.W., 2002. U-Pd geochronology of Palaeoproterozoic rocks in the southern part of the Kedougou-Kéniéba Inlier, Senegal, West Africa: Evidence for diachronous accretionary development of the Eburnean province. Precambrian Research, **118**, 83-99.

Hirdes, W., Davis, D.W., Ludtke, G., Konan, G., 1996. Two generations of Birimian (Paleoproterozoic) colcanic belts in noerteastern Cote d'Ivoire (West Africa): consequences for the Birimian controversy. Precambrian Research, **80**, 173-191.

Leeder, M., 1999. Sedimentology and Sedimentary Basins: From turbulence to tectonics, Blackwell Science Ltd. 592p.

Milesi, J.P., Feybesse, J.L., Ledru, P., Dommanget, A., Ouedraogo, M.F., Marcoux, E., Prost, A., Vinchon, C., Sylvain, J.P., Johan, V., Tegyey, M., Calvez, J.Y., Lagny, P., 1989. West African gold deposits, in their lower Proterozoic lithostructural setting. Chronique de la Recherché Minière, **497**, 3-98.

Naba, S., Lompo, M., Debat, P., Bouchez, J.L., Beziat, D., 2004. Structure and emplacement model for late-orogenic Paleoproterozoic granitoids: the Tenkodogo-Yamba elongated pluton (Eastern Burkina Faso). Journal of African Earth Sciences, **38**, 41-57.

Nesse, W. D., 2000. Introduction to Mineralogy, Oxford University Press. 442p.

Nichols, G., 2009. Sedimentology and stratigraphy, Second edition, Wiley Blackwell, A John Wiley & Sons, Ltd., Publication. 419p.

Nikiema, S., Benkhelil, J., Corsini, M., Bourges, F., Dia, A., Maurin, J-C., 1993. Tectonique transcurrente éburnéenne au sein du craton ouest-africain: exemple du sillon de Djibo (Burkina Faso). Comptes Rendus de l'Académie des Sciences de Paris, Série II, **316**, 661-668.

Pons, J., Barbey, P., Dupuis, D., Léger, J.M., 1995. Mechanisms of pluton emplacement and structural evolution of a 2.1 Ga juvenile continental crust: the Birimian of southwestern Niger. Precambrian Research, **70**, 281–01.

Reading, H.G., 1978. Sedimentary Environments and Facies, Blackwell Scientific Puplications. 569p.

Sawyer, E.W., 2008. Atlas of Migmatites, Special Publication 9, NRC Research Press. 371p.

Spry, A., 1969. Metamorphic Textures, First Edition, Pergamon Press Ltd. 350p.

Tshibubudze, A., Hein, K.A.A., Marquis, P., 2009. The Markoye Shear Zone in NE Burkina Faso. Journal of African Sciences, **55**, 245-256.

Tshibubudze, A., Hein, K.A.A., submitted. Structural setting of gold deposits in the Oudalan-Gorouol greenstone belt east of the Markoye Shear Zone, West African craton. Precambrian Research.

Vernon, R. H., 1976. Metamorphic Processes: Reactions and microstructure development, George Allen & Unwin Ltd. 247p.

Vernon, R.H. and Clarke, G.L., 2008. Principles of Metamorphic Petrology, Cambridge University Press. 446p.

Vidal, M., Delor, C., Pouclet, A., Simeon, Y., Alric, G., 1996. Evolution geodynamique de l'Afrique de l'Ouest 2,2 Ga et 2 Ga: le style «archeen» des ceintures et des ensembles sedimentaires birimiens du nord-est de la C^ote-d'Ivoire. Bulletin Societe Geologique France, **167** (3), 307–319.

Appendix:

Station point data

STN	EASTINGS	NORTHINGS	HOST ROCK TYPE	FEATURE	STR	DIP	DIPD	STRUC TYPE	AZIMUTH	PLUNG
1	805055	1599016	Metagreywacke	Foliation	104	32	N	Lination	064	31
2	806202	1599085	Buckquartz							
3	806198	1599060	Metagreywacke	Foliation	092	46	N	Lineation	072	30
	806198	1599060	Metagreywacke					Lineation	072	29
4	806198	1599017	Metagreywacke	Foliation	092	61	N	Lineation	074	36
	806198	1599017	Metagreywacke					Lineation	072	30
5	806141	1599024	Metagreywacke	Foliation	084	67	N	Lineation	062	22
	806141	1599024	Metagreywacke					Lineation	050	28
6	806121	1599009	Metagreywacke	Foliation	093	67	N			
7	806117	1599020								
8	806082	1599012	Quartz	Foliation	100	74	N			
9	806053	1599001	Metagreywacke	Foliation	083	52	N			
10	806009	1599001	Quartz	Foliation	090	54	N			
11	805980	1599003	Quartz							
12	806003	1598964	Metagreywacke							
13	806000	1598949	Quartz	Foliation	084	67	N	Lineation	062	39
14	806071	1598940	Quartz							
15	806102	1598904	Quartz							
16	805945	1598895	Quartz					Lineation	060	26
17	805996	1598886	Quartz							
18	805998	1598859	Metagreywacke	Foliation	120	70	NE	Lineation	080	24
	805998	1598859	Metagreywacke					Lineation	062	48
	805998	1598859	Metagreywacke					Lineation	052	22
19	805939	1598836	Metagreywacke					Lineation	069	32
20	805211	1599108	Metagreywacke							
21	805218	1599074	Metagreywacke							
22	805221	1599050	Metagreywacke							
23	805231	1599032	Metagreywacke							
24	805220	1599022	Metagreywacke							
25	805254	1599017	Metagreywacke							
26	805244	1598979	Quartz							
27	805272	1598820	Metagreywacke							
28	805381	1598825	Metagreywacke							
29	805403	1598842	Metagreywacke							
30	805442	1598912	Ferocrete							
31	805455	1598912	Ferocrete							
32	805412	1598962	Quartz							
33	805429	1598983	Quartz							
34	805440	1599010	Metagreywacke							
35	805588	1599052	Metagreywacke							
36	805586	1599063	Metagreywacke							
37	805574	1598992	Metagreywacke							
38	805609	1598986	Metagreywacke							
39	805726	1598905	Quartz							

40	805766	1598875	Quartz							
41	805923	1598890	Ferocrete							
42	806221	1599082	Quartz							
43	806006	1598999	Metagreywacke							
44	805934	1599014	Metagritstone							
45	805783	1599018	Metagreywacke							
46	805892	1598855	Metagreywacke							
47	805879	1598887	Quartz							
48	806699	1598927	Metagreywacke	Foliation	090	62	N	Lineation	075	20
	806699	1598927	Metagreywacke						070	31
49	806716	1598958	Metagreywacke	Foliation	077	70	N	Lineation	070	28
	806716	1598958	Metagreywacke						078	22
50	806794	1599018	Metagreywacke							
51	806772	1599045	Metagritstone							
52	806807	1599129	Metagreywacke							
53	806768	1599256	Metagreywacke							
54	806815	1599293	Quartz							
55	806893	1599284	Metagreywacke							
56	806930	1599196	Metagreywacke							
57	806900	1599143	Metagreywacke							
58	806898	1599087	Quartz							
59	806880	1599040	Metagreywacke							
60	806564	1598924	Metagreywacke							
61	806560	1598976	Metagreywacke							
62	806561	1598988	Metagreywacke							
63	806565	1599050	Metagritstone							
64	806041	1599155	Quartz							
65	806019	1599088	Quartz							
66	805930	1599057	Metagreywacke							
67	805247	1599047	Metagreywacke	Foliation	092	61	N	Lineation	059	20
68	805282	1599043	Metagreywacke							
69	805306	1599036	Metagreywacke							
70	805027	1599034	Metagreywacke	Foliation	088	61	N	Lineation	074	17
71	805364	1599083	Metagreywacke							
72	805402	1599029	Metagreywacke	Foliation	080	48	N	Lineation	071	40
73	805405	1599050	Metagreywacke							
74	805442	1599050	Metagreywacke	Foliation	080	50	N			
75	805518	1599057	Metagreywacke	Foliation	084	62	N			
76	805581	1599064	Metagreywacke							
77	805653	1599051	Metagreywacke	Foliation	082	60	N	Lineation	072	32
	805653	1599051	Metagreywacke						073	34
78	805735	1599035	Metagreywacke	Foliation	097	56	N	Lineation	080	20
	805735	1599035	Metagreywacke						048	26
79	805841	1599022	Metagreywacke	Foliation	094	60	N	Lineation	070	16
	805841	1599022	Metagreywacke						050	10
80	805821	1599044	Metagreywacke							
81	805884	1599109	Metagreywacke							
82	805942	1599062	Metagreywacke							

83	805969	1599033	Quartz	Foliation	070	14	N	Lineation	060	18
	805969	1599033	Quartz						065	28
84	806050	1599008	Metagreywacke	Foliation	074	46	N	Lineation	072	21
85	806138	1598943	Quartz	Foliation	079	54	N	Lineation	073	20
	806138	1598943	Quartz					Lineation	068	32
86	806194	1598914	Metagreywacke							
87	806067	1598939	Quartz	Foliation	085	50	N	Lineation	071	28
88	806054	1598953	Metagreywacke	Foliation	078	54	N			
89	805998	1598964	Quartz							
90	805777	1598976	Quartz	Foliation	089	56	N			
91	805577	1598995	Quartz							
92	805363	1598971	Metagritstone							
93	805630	1598914								
94	805680	1598872	Metagritstone	Foliation	080	72	N	Lineation	068	24
95	805577	1598961	Metagritstone	Foliation	080	64	N	Lineation	076	28
96	805452	1598848	Metagritstone					Lineation	065	22
97	805364	1598842	Metagritstone	Foliation	097	60	N	Lineation	072	22
98	806534	1599936	Metagritstone					Lineation	077	30
99	806522	1598936	Metagritstone					Lineation	069	15
100	806617	1598904	Metagritstone					Lineation	071	39
101	806681	1598919	Metagritstone					Lineation	058	30
102	806711	1598921	Metagritstone					Lineation	059	21
103	807959	1599253	Metagritstone	Foliation	066	74	N			
104	808002	1599297	Metagritstone	Foliation	092	78	N			
105	807938	1599296	Metagritstone	Foliation	091	52	N			
106	807808	1599369	Metagritstone	Foliation	092	56	N			
107	807773	1599242	Metagritstone	Foliation	089	62	N	Lineation	065	24
	807773	1599242	Metagritstone					Lineation	082	20
	807773	1599242	Metagritstone					Lineation	082	20
108	807700	1599248	Metagritstone	Foliation	086	60	N			
109	807577	1599261	Metagritstone	Foliation	082	64	N			
110	804853	1599544	Metagreywacke							
111	804942	1599334	Metagritstone							
112	804980	1599343	Metagreywacke							
113	805143	1599302	Buckquartz							
114	805577	1598585	Ferocrete							
115	805599	1598527	Buckquartz							
116	806522	1597097	Ferocrete							
117	806708	1596624	Gabbro							
118	806753	1596587	Buckquartz							
119	806850	1596046	Gabbro							
120	806990	1595853	Gabbro							
121	806994	1595777	Gabbro							
122	807238	1595349	Metagritstone	Foliation	095	50	N			
	807238	1595349	Metagritstone	Foliation	090	40	N			
123	807365	1595079	Quartzite							
124	807448	1594911	Metagreywacke							
125	807582	1594514	Metagreywacke							

126	807800	1594699	Migmatite				
127	807799	1594799	Gneiss				
128	807739	1595431	Metagritstone	Foliation	099	43	N
129	807663	1595687	Gabbro				
130	808996	1595424	Amphibolite	Comp. banding	178	63	E
131	809096	1595391	Amphibolite	Comp. banding	150	88	E
132	809351	1595235	Amphibolite	Comp. banding	051	78	W
133	809542	1595139	Amphibolite				
134	809476	1595416	Gritstone				
135	809420	1595483	Granitic Pegamatite				
136	809540	1595652	Amphibolite				
137	809476	1595707	BIF	Bedding	006	28	N
	809487	1595726	BIF				
	809502	1595790	BIF				
	809454	1595687	BIF				
	809445	1595671	BIF				
	809430	1595666	BIF				
	809314	1595599	BIF				
	809537	1595716	BIF				
	809476	1595616	BIF				
	809316	1595610	BIF				
	809304	1595614	BIF				
138	809334	1595602	BIF	Bedding	137	44	E
139	809277	1595678	BIF	Bedding	168	33	E
140	809276	1595715	BIF	Bedding	069	81	N
	809040	1595900	BIF				
141	809032	1595889	Granitic Pegamatite				
142	809029	1595880	Ferocrete				
143	809002	1595884	Musc Pegmatite				
144	808939	1595914	Metagreywacke	Foliation	065	40	N
	808898	1595891	Metagreywacke	Foliation	059	36	N
145	808881	1595915	Metagreywacke	Foliation	068	40	N
	808826	1595958	Metasiltstone	Foliation	069	38	N
	808826	1595958	Metasiltstone	Foliation	069	44	N
146	808803	1595981	Metagritstone	Foliation	055	35	N
	808803	1595981	Metagritstone	Foliation	048	39	N
	808803	1595981	Metagritstone	Foliation	052	32	N
147	808530	1596381	Granodiorite				
148	808474	1596423	Metagreywacke				
149	809276	1595671	BIF				
	809256	1595699	BIF				
	809203	1595699	BIF				
150	808957	1596017	Metagreywacke	Foliation	050	35	N
151	808908	1596130	Metagritstone	Foliation	062	35	N
152	809020	1596142	Metasiltstone				

153	809084	1596197	Metagreywacke				
154	809020	1596288	Metagritstone				
155	808953	1596327	Metagreywacke				
156	808860	1596225	Buckquartz				
157	808656	1595846	Metagreywacke				
158	808667	1595814	Metagreywacke	Foliation	065	39	N
	808667	1595814	Metagreywacke	Foliation	070	38	N
159	808757	1595770	Metagritstone	Foliation	070	31	N
160	808822	1595811	Metagritstone	Foliation	084	56	N
161	808774	1595802	Metasiltstone				
162	808639	1595705	Metasiltstone				
	808592	1595664	Metasiltstone				
163	808633	1595675	Metagritstone	Foliation	070	48	N
164	808566	1595568	Metagreywacke	Foliation	070	35	N
	808566	1595568	Metagreywacke	Foliation	071	40	N
165	808437	1595312	Metasiltstone	Foliation	073	38	N
	808437	1595312	Metasiltstone	Foliation	075	40	N
166	808381	1595324	Metagreywacke	Foliation	066	30	N
	808381	1595324	Metagreywacke	Foliation	077	30	N
167	808315	1595440	Metagritstone	Foliation	081	38	N
168	808060	1595418	Metagritstone	Foliation	091	40	N
169	808035	1595331	Metagreywacke	Foliation	094	35	N
	808035	1595331	Metagreywacke	Foliation	085	45	N
	808035	1595331	Metagreywacke	Foliation	091	40	N
170	808052	1595297	Metasiltstone	Foliation	100	60	N
	808052	1595297	Metasiltstone	Foliation	097	48	N
	808052	1595297	Metasiltstone	Foliation	082	36	N
171	807943	1594952	Gneiss				
172	808161	1594860	Gneiss				
173	808597	1594701	Amphibolite				
174	809420	1595482	Amphibolite	Comp. banding	018	66	W
	809409	1595462	Amphibolite	Comp. banding	045	71	W
175	808298	1595193	Amphibolite	Comp. banding	033	77	E
	809303	1595250	Amphibolite	Comp. banding	029	17	W
176	809270	1595182	BIF	Bedding	036	56	W
	809243	1595172	BIF	Bedding	016	25	W
177	809100	1595203	Amphibolite	Comp. banding	150	67	E
178	809203	1595119	Amphibolite	Comp. banding	072	73	N
179	809199	1595108	Amphibolite	Comp. banding	008	75	E
180	808895	1594917	Amphibolite	Comp. banding	066	79	S
	808857	1594876	Amphibolite				
	808807	1594843	Amphibolite				

	808761	1594762	Amphibolite				
	808701	1594718	Amphibolite				
181	808763	1594442	Iron gossan	Foliation	041	50	N
182	808142	1594396	Amphibolite	Comp. banding	134	73	E
183	808138	1594408	Amphibolite	Comp. banding	069	65	N
	807964	1594363	Amphibolite	Comp. banding	052	64	N
	807846	1594381	Amphibolite	Comp. banding	088	74	N
	807663	1594388	Amphibolite	Comp. banding	077	61	N
184	808254	1594788	Migmatite				
	808297	1594792	Migmatite				
	807779	1594673	Migmatite				
185	808114	1594861	Migmatite				
	808124	1594816	Migmatite				
	808244	1594836	Migmatite				
	808244	1594869	Migmatite				
186	808212	1594910	Metagreywacke				
	807734	1594767	Metagreywacke				
187	807943	1594948	Migmatite				
188	807834	1594734	Migmatite				
189	807749	1594800	Metagreywacke				
190	807749	1595342	Metagreywacke	Foliation	089	34	N
	807751	1595404	Metagreywacke	Foliation	090	45	N
191	806827	1599022	Metagritstone	Foliation	062	51	N
	806798	1599046	Metagritstone	Foliation	067	55	N
192	806784	1599052	Fe-oxide sandstone	Foliation	081	49	N
193	806739	1599129	Metagreywacke	Foliation	076	64	N
194	808642	1599445	Metagreywacke				
195	808268	1600024	Buckquartz				
196	808405	1599441	Metagreywacke				
197	808438	1599377	Metagritstone	Foliation	076	79	N
198	808444	1599304	Buckquartz				
199	808597	1599087	Gabbro				
200	808491	1598854	Metagreywacke				
201	808429	1598782	Gabbro				
	808375	1598842	Gabbro				
202	808432	1598662	Gabbro				
203	808744	1598754	Gabbro				
204	809172	1597524	Buckquartz				
	809198	1597642	Buckquartz				
205	809208	1596591	Buckquartz				
206	808452	1596352	Granodiorite				
207	807985	1596018	Gabbro				
	807988	1596010	Gabbro				
	807969	1596036	Gabbro				
	807993	1595975	Gabbro				

208	807767	1596391	Buckquartz				
209	806244	1598959					
210	807074	1599392	Metagreywacke	Foliation	050	59	N
	807091	1599360	Metagreywacke	Foliation	055	59	N
	807111	1599339	Metagreywacke	Foliation	051	65	N
	807087	1599279	Metagreywacke	Foliation	073	52	N
	806978	1599296	Metagreywacke	Foliation	065	78	N
	807475	1599360	Metagreywacke	Foliation	068	67	N
	807061	1599242	Metagreywacke				
211	807142	1599199	Metagreywacke				
212	807213	1599216	Metagritstone	Foliation	065	55	N
	807286	1599205	Metagritstone	Foliation	063	46	N
213	807223	1599121	Metagritstone	Foliation	072	53	N
	807475	1599214	Metagritstone	Foliation	070	62	N
214	807503	1598746	Sand covered				
	808162	1598394	Sand covered				
215	807625	1598588	Ferocrete				
	808047	1596880	Ferocrete				
	807745	1595892	Ferocrete				
	807131	1596084	Ferocrete				
216	808009	1599034	Buckquartz				
217	808306	1599036	Gabbro				
	808336	159872	Gabbro				
	808109	1598464	Gabbro				
218	808352	1598805	Gabbro				
219	808371	1598671	Gabbro				
	808404	1598617	Gabbro				
220	807807	1597913	Farm land				
	807141	1596441	Farm land				
	808127	1597222	Farm land				
	807722	1598250	Farm land				
221	807571	1595415	Metagritstone	Foliation	075	40	N
	807571	1595415	Metagritstone	Foliation	079	42	N
222	807668	1595679	Gabbro				
	807627	1595694	Gabbro				
223	807288	1596071	Infered gabbro intusion				
224	807080	1597416	Farm land				
225	807025	1597850	Infered gabbro intusion				
226	806996	1598023	Road				
227	806470	1597610	Gabbro				
228	806552	1597217	Gabbro				
	806563	1597224	Gabbro				
229	806590	1596361	Metagreywacke				
230	806534	1596334	Gabbro				
231	806435	1595874	Metagreywacke	Foliation	032	60	E
	806490	1595944	Metagreywacke	Foliation	039	67	E
	806434	1595703	Metagreywacke	Foliation	030	75	E
	806448	1595760	Metagreywacke				

232	806242	1596067	Gabbro
	806196	1596054	Gabbro
	806219	1596003	Gabbro
	806225	1596019	Gabbro
233	805837	1596825	Metagreywacke
234	805623	1597173	Ferocrete
235	808826	1594551	Iron gossan
	808924	1594578	Iron gossan
	808991	1594473	Iron gossan